

**CLOSED CHAMBER WELL TEST
INCLUDING
FRICTIONAL EFFECTS**

**A REPORT
SUBMITTED TO THE DEPARTMENT OF PETROLEUM ENGINEERING
OF STANFORD UNIVERSITY
IN PARTIAL FULFILLMENT OF THE REQUIREMENTS
FOR THE DEGREE OF
MASTER OF SCIENCE**

by

Beatriz del Socorro Salas

August, 1986

ABSTRACT

Frictional effects were included in the closed chamber well test model in order to develop a more general solution for the closed chamber well test. Superposition of the cumulative influx, constant pressure solution of the radial diffusivity equation is used to overcome the limitations and difficulties resulting from solving the diffusivity equation in the presence of changing wellbore storage and frictional effects.

A sensitivity study was performed to analyze the influence of different tool and reservoir parameters on the closed chamber well test in the presence of frictional effects. Frictional effects significantly affect the early time pressure response of the closed chamber well test.

The superposition model was also improved by using variable time steps, hence, increasing the computation efficiency of the model.

TABLE OF CONTENTS

	<u>Page</u>
ABSTRACT	i
TABLE OF CONTENTS	ii
LIST OF FIGURES	iv
LIST OF TABLES.....	v
1. INTRODUCTION	1
2. LITERATURE SURVEY	4
3. CLOSED CHAMBER PRESSURE RESPONSE ANALYSIS	6
3.1. Fluid Flow in Pipes	6
3.2. Frictional Head Loss.....	8
3.3. Closed Chamber Well Test Model	10
3.3.1. Without Frictional Effects.....	10
3.3.2. With Frictional Effects.....	14
3.3.2.1. Fixed Time Step.....	15
3.3.2.2. Variable Time Steps - Interpolator.....	15
4. VERIFICATION OF THE MODEL INCLUDING FRICTION EFFECTS	18
4.1. Verification of Basecase Results	18
4.2. Basecase Analysis.....	20

5. SENSITIVITY STUDY	29
5.1. Effect of Wellbore Skin.....	29
5.2. Effect of Initial Reservoir Pressure	39
5.3. Effect of Chamber Diameter	46
5.4. Effect of Roughness	53
5.5. Effect of Initial Chamber Pressure	56
6. CONCLUSIONS AND RECOMMENDATIONS.....	60
NOMENCLATURE	63
REFERENCES	66
APPENDIX 1. COMPUTER PROGRAM	68
APPENDIX 2. NUMERICAL VALUES FOR THE BASECASE.....	81

LIST OF FIGURES

	<i>Page</i>
Figure 1: Schematic Representation of the Closed Chamber Equipment	3
Figure 2: Definition of Variables for the Closed Chamber Model	13
Figure 3: Bottom Hole Pressure Obtained with 2 Different Models	17
Figure 4: Frictional Pressure Drop Obtained with 2 Different Models	17
Figure 5: Bottom Hole Pressure for Basecase Without Friction	19
Figure 6: Basecase Without Friction	23
Figure 7: Basecase With Friction	23
Figure 8: Bottom Hole Pressure for Basecase With and Without Friction	24
Figure 9: Chamber Pressure for Basecase With and Without Friction	24
Figure 10: Elevation Pressure for Basecase With and Without Friction	25
Figure 11: Frictional Pressure Drop for Basecase	25
Figure 12: Oil Flowrate for Basecase With and Without Friction	26
Figure 13: Early Time Plot for Basecase With and Without Friction	27
Figure 14: Late Time Plot for Basecase With and Without Friction	28
Figure 15: Bottom Hole Pressure for Different Skins	31
Figure 16: Frictional Pressure Drop for Different Skins	31
Figure 17: Oil Flowrate for Different Skins	32
Figure 18: Early Time Plot for Different Skins	33
Figure 19: Late Time Plot for Different Skins	34
Figure 20: Bottom Hole Pressure for Skin=2 With and Without Friction	35
Figure 21: Bottom Hole Pressure for Skin=5 With and Without Friction	35
Figure 22: Early Time Plot for Skin=2 With and Without Friction	36
Figure 23: Early Time Plot for Skin=5 With and Without Friction	37
Figure 24: Late Time Plot for Skin=2 With and Without Friction	38
Figure 25: <u>Late Time Plot</u> for Skin=5 With and Without Friction	38

Figure 26: Bottom Hole Pressure for Different Initial Reservoir Pressures	40
Figure 27: Frictional Pressure Drop for Different Initial Reservoir Pressures	40
Figure 28: Oil Flowrate for Different Initial Reservoir Pressures	41
Figure 29: Early Time Plot for Different Initial Reservoir Pressures	42
Figure 30: Late Time Plot for Different Initial Reservoir Pressures	43
Figure 31: Bottom Hole Pressure for $p_i=3000$ psig	43
Figure 32: Early Time Plot for $p_i=3000$ psig	44
Figure 33: Late Time Plot for $p_i=3000$ psig	45
Figure 34: Bottom Hole Pressure for Different Chamber Diameters	47
Figure 35: Frictional Pressure Drop for Different Chamber Diameters	47
Figure 36: Bottom Hole Pressure for $D_{ch}=4.00$ inches	48
Figure 37: Oil Flowrate for Different Chamber Diameters	48
Figure 38: Early Time Plot for Different Chamber Diameters	49
Figure 39: Late Time Plot for Different Chamber Diameters	50
Figure 40: Early Time Plot for $D_{ch}=4.00$ inches	51
Figure 41: Late Time Plot for $D_{ch}=4.00$ inches	52
Figure 42: Bottom Hole Pressure for Different Roughness	54
Figure 43: Frictional Pressure Drop for Different Roughness	54
Figure 44: Oil Flowrate for Different Roughness	55
Figure 45: Bottom Hole Pressure for Different Initial Chamber Pressures	57
Figure 46: Frictional Pressure Drop for Different Initial Chamber Pressures	57
Figure 47: Early Time Plot for Different Initial Chamber Pressures	58
Figure 48: Late Time Plot for Different Initial Chamber Pressures	59

LIST OF TABLES

Table 1: Basecase Parameters	22
------------------------------------	----

1. INTRODUCTION

The closed chamber well test is a suitable **method** to identify and Sample formation fluids, **as** well as to determine oil reservoir parameters required for estimating productivity.

Closed chamber well testing is used in the petroleum industry in the **form** of backsurge perforation cleaning (*Simmons* (1985), *Simmons* (1986)). **As** shown in Figure 1, the equipment used for backsurge operations includes: a work string composed of two remote controlled valves, a temporary packer, and a pressure recorder. The assembly is run into the wellbore with an enclosed chamber formed between the upper and the lower surge valves. The increase in the hydrostatic pressure is recorded as the assembly is run into the well. When the packer is set the completion fluid overbalance is relieved, and the bottom hole pressure becomes equal to the static initial reservoir pressure. When the lower valve is opened the drawdown is obtained, **as** the formation sandface is exposed to a minimum pressure, and fluids **are** produced. Then, the fluid level rises and the bottom hole pressure increases until it reaches the static reservoir pressure. Finally, the upper valve *is* opened, the packer released and ~~the~~ bottom hole pressure returns to an overbalance.

The closed chamber well test is similar to **a** conventional drillstem test; moreover, it is a generalized form **of** the drillstem test known **as** slug test. The closed chamber well test involves liquid level changes in the wellbore as a result **of** the instantaneous removal of a specific amount of liquid **from** the wellbore. The main difference between ~~the~~ closed chamber test and the slug test is wellbore storage. The slug test wellbore storage is constant, related either **to** fluid level rise or to fluid compression in a fixed volume. The closed chamber test wellbore storage varies **from** being controlled by fluid level rise, to fluid compression in a changing volume. **In** a closed chamber test, the initial wellbore storage is high and reduces **dur-**ing the test, **as** the chamber gas compresses above the liquid column.

The variable wellbore storage and the presence of frictional and momentum effects throughout the test, make the closed chamber well test problem non-linear and difficult to solve

analytically. Hence, numerical techniques **are** required to overcome the limitations and difficulties resulting from these non-linearities.

This study was performed in order to develop a more general solution for the closed chamber well **test** by including frictional effects in the closed chamber well test model developed by **Simmons (1985)** **as** well as improving the efficiency **of** the model by using variable time steps.

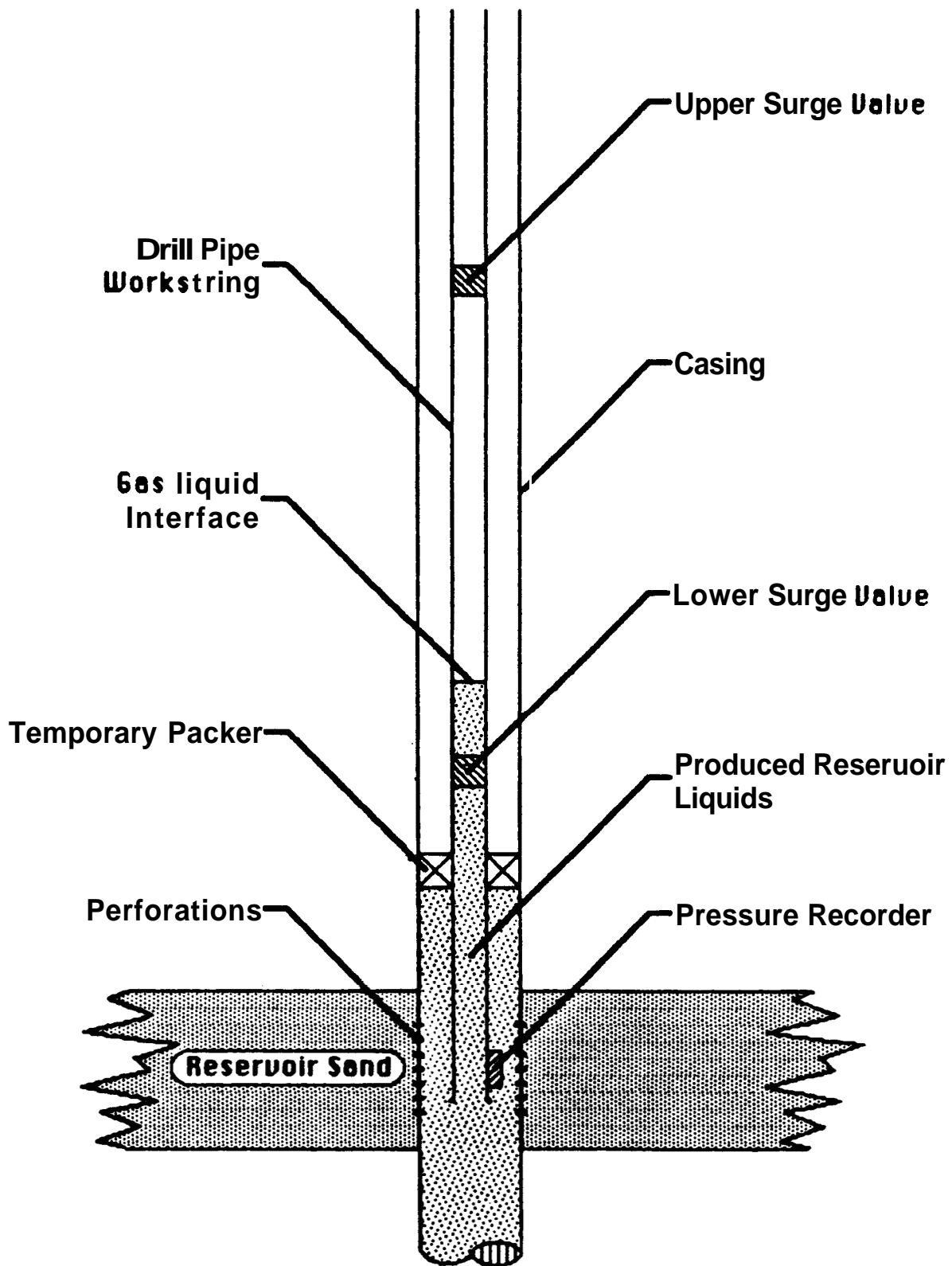


Figure 1: Schematic Representation of the Closed Chamber Equipment (after *Simmons* (1985), *Simmons* (1986))

2 LITERATURE SURVEY

The first application of slug test analysis was presented by *Ferris and Knowles* (1954), who proposed the instantaneous slug test method for determining the transmissivity of an aquifer. They analyzed late time data considering the instantaneous line source response, but neglected the effects of wellbore storage and **skin**.

Cooper, Bredehoeft, and Papadopoulos (1967), presented a solution for the variation in the liquid level when a slug test is performed. They considered wellbore storage in the analysis, and proposed using type curves for determining reservoir transmissivity.

After that, *Ramey and Agarwal* (1972) presented the slug test solution including the effects of wellbore storage and skin, but momentum, friction, phase change and wellbore fluid compressibility effects were neglected. *Ramey, Agarwal, and Martin* (1975), presented **type** curves for the slug test. **Three** kinds of curves were developed: a) log-log early time, b) semi-log intermediate time, and **c)** log-log late time. These curves combine skin effect as well as wellbore storage into a correlating parameter that may be determined **from** a type curve match.

A theory for analyzing closed chamber well tests was presented by *Alexander* (1977) and *Marshall* (1978). They suggested using the results obtained by performing a closed chamber test to monitor the initial flow period **of** the drillstem test, **as well as** to identify and measure formation properties.

As **an** extension of the **general** slug test solution, *Shinohara* (1980), presented a mathematical solution to **analyze** data from closed chamber tests. The solution he proposed can **be** applied for **the** closed chamber test problem except when the volume of the closed chamber **is** very **small**, or there is a considerable difference between the **initial** pressure of the closed chamber and **the** atmospheric pressure. The solution was obtained based on a wellbore momentum balance. Some of the assumptions adopted in the analysis were that the wellbore friction, the compressibility of the liquid in the wellbore, and **mass** transfer between liquid and **gas** were negligible. Also, ideal chamber gas behavior was assumed.

After that, *Saldana (1983)* proposed a mathematical solution to describe the flow phenomena occurring during a slug test, a drillstem test, or a closed chamber test. The solution was obtained by applying a momentum balance equation to ~~the~~ liquid in the wellbore including gravitational, inertial, and frictional effects on the fluid column. *Saldana* also assumed ideal gas behavior in the analysis.

Simmons (1985) developed a closed chamber test model, obtained by ~~the~~ superposition of the constant pressure cumulative influx solution to ~~the~~ radial diffusivity equation. In his approach he considered real **gas** compressibility effects, but the effects of friction and momentum were not included. In addition, no mass exchange and incompressible wellbore liquids were assumed.

Based on the results of Simmons's approach, *Simmons and Sageev (1985)* presented a method **for** analyzing backsurge pressure data to determine the reservoir transmissivity and the Hurst skin effect. In a paper to be presented **in 1986**, *Simmons* presents a new method **for** analyzing closed chamber tests. In **this** method, the recorded chamber pressures are differentiated, yielding the instantaneous sandface rate. Then, the superposition model of constant rates is invoked allowing the determination **of** formation transmissivity, and the variation of wellbore skin with time. However, we still lack **a method for** reproducing the bottom hole pressure including the frictional and momentum effects.

3. CLOSED CHAMBER PRESSURE RESPONSE ANALYSIS

3.1. Fluid Flow in Pipes

The pressure drop for a fluid flowing between two points, (1 and 2), in a pipe is expressed by:

$$144 \left[p_1 v_1 + \int_{v_1}^{v_2} p dv - p_2 v_2 \right] = \frac{g}{g_c} (z_2 - z_1) + \alpha \frac{(V_2^2 - V_1^2)}{2g_c} + h_f \frac{g}{g_c} \quad (1)$$

where:

- p = pressure
- v = specific volume ($v = 1/\rho_f$)
- z = elevation
- V = average fluid velocity
- h_f = frictional head loss
- α = kinetic energy correction term
- g = acceleration of gravity
- g_c = conversion factor

For liquids, assuming that the density remains constant, equation (1) becomes the generalized Bernoulli equation for flowing liquids in a pipe:

$$144 \frac{p_1 - p_2}{\rho_f} = \frac{g}{g_c} (z_2 - z_1) + \alpha \frac{(V_2^2 - V_1^2)}{2g_c} + h_f \frac{g}{g_c} \quad (2)$$

where:

- ρ_f = fluid density

Equation (2) can be expressed as

$$- 144 \frac{\Delta p}{\rho_f} = \frac{g}{g_c} \Delta z + \frac{\alpha \Delta(V^2)}{2g_c} + \frac{g}{g_c} h_f \quad (3)$$

where:

Δp = pressure change

$\Delta(V^2)$ = change in velocity terms

Δz = change in elevation

The kinetic energy correction factor, α , is usually set equal to unity (*Benedict, 1980*). Then, when the pipe diameter is constant, the total pressure drop can be calculated from equation (3) as

$$-(\Delta p)_{total} = \frac{1}{144} \rho_f \frac{g}{g_c} \Delta z + \frac{1}{144} \rho_f \frac{g}{g_c} h_f \quad (4)$$

Equation (4) is of the general form:

$$-(\Delta p)_{total} = (\Delta p)_{elevation} + (\Delta p)_{friction} \quad (5)$$

3.2. Frictional Head Loss

The head loss due to friction in a pipe is defined by the Darcy-Weisbach equation as

$$h_f = f \frac{L}{D} \frac{V^2}{2g} \quad (6)$$

where:

f = friction factor

L = length

D = inside pipe diameter

The frictional pressure drop in Equation (5) is then given by

$$(\Delta p)_{friction} = \frac{1}{144} \rho_f \frac{g}{g_c} h_f = \frac{1}{144} \rho_f f \frac{L}{D} \frac{V^2}{2g_c} \quad (7)$$

Expressing (6) as a function of the flowrate, q , we have

$$h_f = 8 f \frac{L q^2}{\pi^2 D^5 g} \quad (8)$$

Substituting Equation (8) in Equation (7), yields the frictional pressure drop expressed as a function of the flowrate

$$(\Delta p)_{friction} = \frac{8}{144} \rho_f f \frac{L q^2}{\pi^2 D^5 g_c} \quad (9)$$

The friction factor, f , as presented by *Moody (1944)* is a function of two dimensionless parameters:

- the relative roughness, e/D , where e is a dimensional quantity that represents the absolute roughness, and

- the Reynolds number,

$$Re = \frac{\rho_f V D}{\mu} \quad (10)$$

where μ is the viscosity of the fluid in *lbm/ft-sec*.

The Reynolds number is dimensionless but may be expressed in oilfield **units** as

$$Re = \frac{13033 q_o (bbl/D)}{\mu_o (cp) D (inches) (131.5+API)} \quad (11)$$

The Moody friction factors are also defined according to the flow regime:

- Laminar zone ($0 < Re \leq 2000$)

$$f = 64/Re \quad (12)$$

- Critical zone ($2000 < Re \leq 4000$)

$$f = 0.5/Re^{0.3} \quad (13)$$

- Transition zone ($4000 < Re \leq (200D/e)^{1.16}$)

$$1/\sqrt{f} = 1.14 - 2 \log(e/D + 9.34/Re\sqrt{f}) \quad (14)$$

- Turbulent zone ($Re > (200D/e)^{1.16}$)

$$1/\sqrt{f} = 1.14 - 2 \log(e/D) \quad (15)$$

An iterative calculation is required to evaluate the Moody friction factor in the transition zone (Equation (14)).

33. Closed Chamber Well Test Model

3.3.1. Without Frictional Effects

Simmons (1985) developed a model for analyzing the pressure response for the closed chamber well test. The model presented by **Simmons** uses superposition, hence, simplifying the solution of the diffusivity equation in the presence of changing wellbore storage. The net influx at a given time step is calculated by using superposition of the cumulative influx, constant pressure solution of the radial diffusivity equation.

The dimensionless radial diffusivity equation is expressed by

$$\frac{\partial^2 p_D}{\partial r_D^2} + \frac{1}{r_D} \frac{\partial p_D}{\partial r_D} = \frac{\partial p_D}{\partial t_D} \quad (16)$$

where the dimensionless time, t_D , and dimensionless radius, r_D , are defined as

$$t_D = \frac{73.25 \times 10^{-9} kt}{\phi \mu c_i r_w^2} \quad (17)$$

$$r_D = \frac{r}{r_w} \quad (18)$$

and the dimensionless pressure, p_D , for a constant pressure inner boundary is given by

$$p_D = \frac{P_i - P_{wf}}{P_i - P_o} \quad (19)$$

The assumptions considered in the development of the model were:

- a. There is no mass exchange between the produced liquids and the chamber gas.
- b. Incompressible wellbore liquids.
- c. Negligible momentum and frictional effects.

- d. The flowrate during the test period is not impeded by critical flow.
- e. Only liquid is produced from the reservoir during the test.
- f. The reservoir behaves as an infinite homogeneous radial system of isotropic properties during the test period.
- g. Negligible gradients of pressure and temperature with respect to depth in the gas column.

The closed chamber model discretizes the pressure response into constant pressure intervals and assumes that the pressure at the beginning of the time step remains constant during the time step. By using superposition of the cumulative influx, constant pressure solution of the radial diffusivity equation, the net influx after N time steps is calculated as

$$N_p = \beta [p_i - p_o] Q_D(N\Delta t_D) - \beta \sum_{j=1}^{N-1} \left[[p_j - p_{j-1}] Q_D([N-j]\Delta t_D) \right] \quad (20)$$

where N_p is the fluid produced (in *bbls*) after N time steps, Δt_D is the dimensionless time step, evaluated based on the time step Δt , and β is a constant of proportionality equal to

$$\beta = 1.119\phi h c_f r_w^2 \quad (21)$$

Q_D is the dimensionless cumulative influx defined as

$$Q_D = \frac{Q}{1.119\phi h c_f r_w^2 (p_i - p_{wf})} \quad (22)$$

and is evaluated by inverting the dimensionless Laplace solution presented by *Da Prat* (1981)

$$\bar{Q}_D = \frac{\sqrt{s} K_1(\sqrt{s})}{s^2 [K_0(\sqrt{s}) + S \sqrt{s} K_1(\sqrt{s})]} \quad (23)$$

where K_0 and K_1 are the zero and first order modified Bessel functions of the second kind.

From the cumulative influx, the fluid level X , shown in Figure 2, is calculated as

$$X = L_{ci} + \frac{N_p}{A_{ch}} \quad (24)$$

where:

L_{ci} = initial fluid level

A_{ch} = area of the chamber

and by assuming isothermal gas compression the chamber pressure is calculated as

$$p_{ch} = \frac{p_{ch_i} [L_c - L_{ci}] Z}{[L_c - X] Z_i} \quad (25)$$

where:

p_{ch_i} = initial chamber pressure

p_{ch} = chamber pressure

Z_i = initial compressibility factor

Z = compressibility factor

Assuming negligible momentum and frictional effects, the bottom hole pressure is calculated as

$$p_{wf} = p_{ch} + \frac{1}{144} \rho_f \frac{g}{g_c} X \quad (26)$$

where:

p_{wf} = bottom hole flowing pressure

p_{ch} = chamber pressure

and the second term in the right hand side is the hydrostatic pressure of the liquid column.

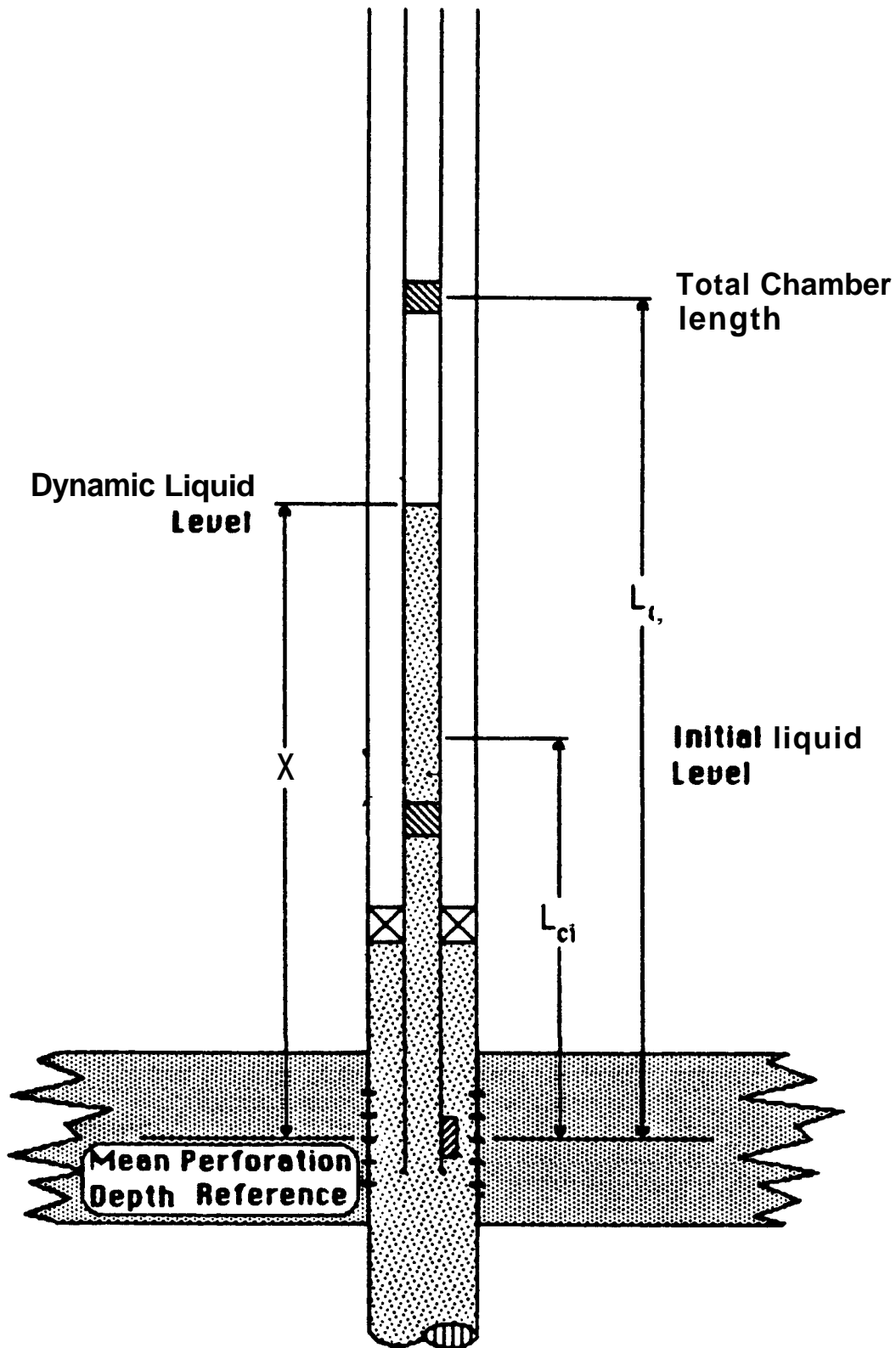


Figure 2: Definition of Variables for the Closed Chamber Model (after *Simmons* (1985), *Simmons* (1986))

33.2. With Frictional Effects

Starting with the closed chamber well test model presented in the preceding section, and neglecting momentum effects, the frictional effects can be included in the model. The friction head changes with time until the fluid stabilizes at the initial static liquid level. By using Simmons's model, assuming that the pressure at the beginning of the time step remains constant during the time step, and taking the average rate and the maximum value of ΔX per time step, the pressure response can be generated for each time step.

The frictional pressure drop is:

$$h_f = 8f \frac{(X+\Delta X) q^2}{\pi^2 D^5 g} \quad (27)$$

The oil flowrate changes during the test, and is a function of the bottom hole pressure. For the constant pressure solution of the radial diffusivity equation, the fluid influx rate at the end of a period of interest can be calculated by first determining the corresponding fluid influx terms and approximating their time derivative by dividing the difference between each two successive values by the corresponding difference in absolute time (Chatas, 1953).

That means, the average oil flowrate during the time step j is:

$$q_j = \frac{N_{p_j} - N_{p_{j-1}}}{t_j - t_{j-1}} \quad (28)$$

Then, the bottom hole flowing pressure considering friction is:

$$p_{wf} = p_{ch} + \frac{1}{144} \rho_f \frac{g}{g_c} (X+\Delta X) + \frac{8}{144} \rho_f f \frac{(X+\Delta X) q^2}{\pi^2 D^5 g_c} \quad (29)$$

Equation (29) expresses the pressure response during the closed chamber well test, taking into account the frictional effects. The calculation of the pressure response by using the model presented in section 3.2., but including the frictional effects, implies that the assumptions esta-

blished in the development of the model also apply in this case.

3.3.2.1. Fixed Time Step

The computer program for the closed chamber well test model, including frictional effects, is presented in Appendix 1. Generally, when using constant time steps, an extremely small time step is required to represent accurately the chamber pressure **rise** and to avoid numerical over shooting above the upper surge valve due to excessive variation of the fluid level. Therefore, to calculate the pressure response over a reasonable interval of time requires a large number of time steps; that implies, unreasonable amount of computer time.

Simmons recommended to improve the superposition model **by** using variable time **steps**, such that the amount of numerical computations be decreased. For this study, a new model with variable time steps was developed. This model is described in the next section.

3.3.2.2. Variable Time Steps - Interpolator

To increase the efficiency of the superposition model a new program that uses variable time steps was developed. The computer program of the closed chamber model with variable time steps is presented in Appendix 1.

The new model allows the use of different time increments along the closed chamber well test. For instance, a larger time increment is used when the chamber pressure is insignificant compared to the reservoir pressure; then, when the fluid level approaches the upper surge valve the time increment is reduced to avoid over shooting above the upper surge valve; finally, larger time increments are used when the chamber pressure has increased close to **its** final **pressure**.

The evaluation of the net influx at a given time by using superposition requires the calculation of the dimensionless cumulative influx (Equation **22**) for all combinations **of the** previous time steps. When variable time steps are used, new dimensionless cumulative influx values

have to be obtained for each pressure change in all the pressure history for every time **step**. **To** calculate these dimensionless values by inverting the dimensionless Laplace solution (Equation **23**) would be a disadvantage and the computational time will increase instead of decrease. To avoid **this** problem an interpolator was developed. **This** interpolator interpolates between two successive values in a given table that contains the dimensionless cumulative influx values for different dimensionless time values. Thus, for a given dimensionless time the interpolator computes the closest lower entry in the table, and interpolates between **this** and the following entry in the table. The interpolator subroutine is presented in Appendix **1**.

To check the new program, the closed chamber well test was analyzed for a specific case with the two models: with a fixed time **step** and with variable time steps. **One of** the cases studied in the sensitivity study, that will **be** presented later in section **5**, was chosen. The selected case corresponds to a skin value **of 2** and zero initial fluid level.

Figures **3** and **4** show the comparison between the results obtained with the two models. Figure **3** presents the bottom hole flowing pressure response and Figure **4** presents the frictional pressure drop. The dotted Curves in both figures represent the response obtained with a fixed time step, and the continuous curves correspond to the response with variable time **steps**. According to these figures, the pressure response obtained with both models is identical. Moreover, **only** 1000 time steps were required with variable time steps, while 10000 time steps were used with a fixed time step (0.01 seconds in **this** case). That means, that using the new program reduced the number of computations and CPU time **by** a factor of 10.

The new model including variable time **steps is** an interactive program, in which the time steps **are** chosen **according** to the development of the pressure response. **This** model could be improved **by** allowing the computer to select the time step during the well test. Some important facts should **be** considered in such a model: the oil flowrate continuously decreases during **the** test, and the rate of change in the bottom hole flowing pressure **has to be** maintained within a tolerance range avoiding the over shooting above the upper surge valve.

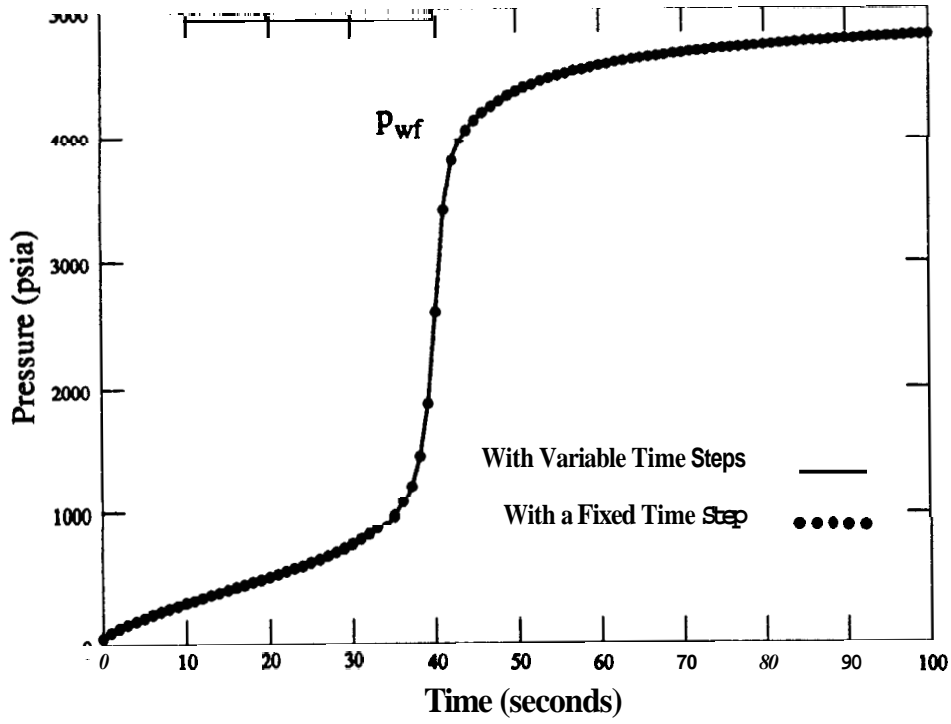


Figure 3: Bottom Hole Pressure Obtained with 2 Different Models

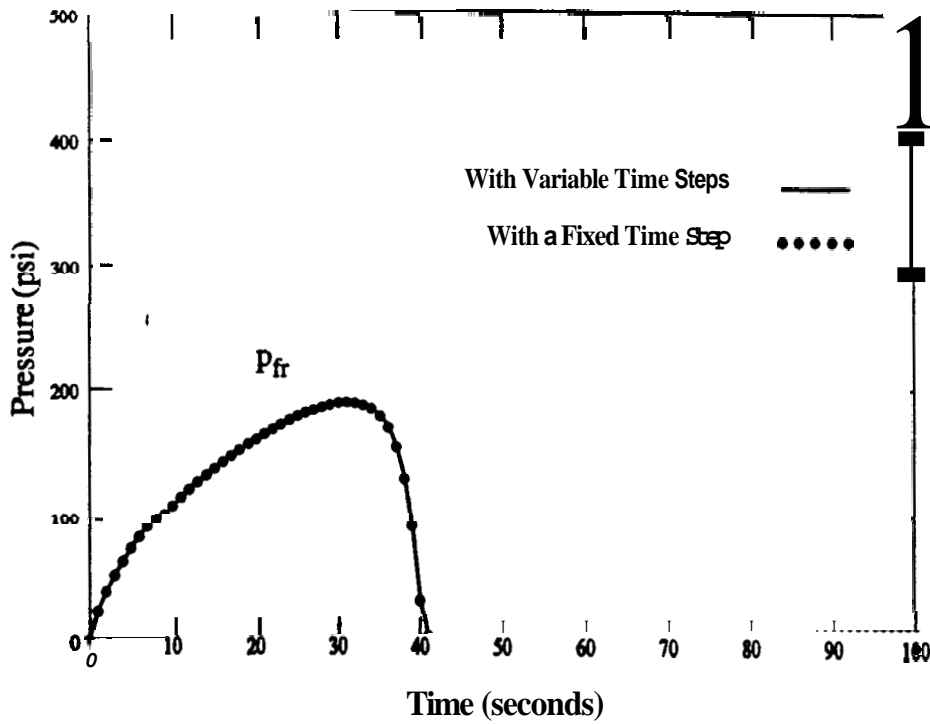


Figure 4: Friction Pressure Drop Obtained with 2 Different Models

4. VERIFICATION OF THE MODEL INCLUDING FRICTION EFFECTS

4.1 .Verification of Basecase Results

Since the difference between the model presented in **this** study and Simmons's lies in the consideration of frictional effects, the new model can be tested by generating Simmons's basecase for no friction conditions in the tubing.

The basecase response that will be explained **in** next section was obtained by using an absolute roughness factor, **e**, of zero. In other words, it was assumed that the frictional pressure drop during the test **is** always zero. Figure **5** presents the bottom hole flowing pressure response obtained with the **two** models. The continuous line represents the pressure response generated with Simmons's model. The dotted line corresponds to the pressure response calculated with the new model, assuming no frictional effects. According to **this** figure, **both** responses **are** identical. Hence, the new model accurately duplicates Simmons's results when the frictional pressure **drop is** neglected in the calculation of the closed chamber pressure response.

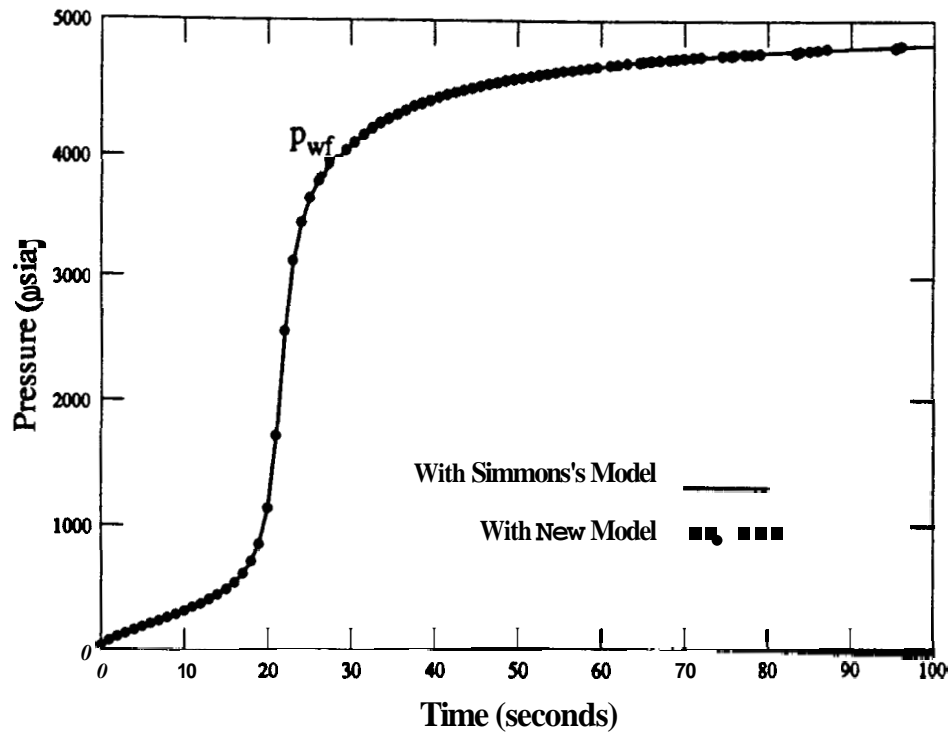


Figure 5: Bottom Hole Pressure for Basecase Without Friction

42. Basecase Analysis

In **this** section we describe the basecase for the parameter investigation that will follow. The basecase described by **Simmons** consisted of zero skin and 100 feet of initial fluid cushion in the well above the lower valve. Since in **this** study the momentum effects in the wellbore were not considered, the basecase was changed so that there is no initial fluid level in the wellbore above the lower valve. More than that, for **this** study the momentum effects of the fluid between the lower valve and the formation were not considered. In other words, the model assumes that the lower valve is positioned opposite the tested zone. All the other parameters such as chamber length, initial chamber pressure, and fluid gravity are the same as were presented by **Simmons**. Table 1 presents the parameters of the basecase.

Figure 6 presents the closed chamber pressure response for the new basecase, without initial fluid level, and without wellbore frictional effects. There are ~~three~~ curves in Figure 6. The uppermost curve represents the bottom hole pressure response, and is the sum of the two other curves: the hydrostatic fluid pressure drop and the chamber pressure. The hydrostatic pressure drop curve represents the fluid level rise after the lower surge valve is opened. As the chamber gas compresses, an abrupt rise in the bottom hole flowing pressure is observed. The difference between the chamber pressure and the bottom hole flowing pressure is the hydrostatic pressure drop of the fluid column, neglecting momentum and frictional effects.

Figure 7 illustrates the closed chamber pressure response for the basecase, without initial fluid level, but including wellbore frictional effects. In **this figure**, in addition to the three curves shown in Figure 6, a fourth curve is present that represents the frictional pressure drop in the wellbore. The bottom hole flowing pressure in **this** case corresponds to the sum of the frictional pressure drop, the hydrostatic fluid pressure drop and the chamber pressure. As in the basecase without friction, the abrupt rise in the bottom hole pressure is due to the rapid compression of the chamber gas. The separation between the bottom hole pressure and the chamber pressure is given in **this case** by the sum of the hydrostatic pressure drop and the frictional pressure drop. After about 25 seconds, when the friction pressure drop reduces to zero,

the difference is given only by the hydrostatic pressure drop like in the basecase without friction.

Figure 8 shows the bottom hole pressure response for the basecase with and without friction. As can be observed in this figure, during the first 20 seconds of the test the bottom hole pressure with friction is larger than the bottom hole pressure without friction. At this time the two curves overlap. After that, the bottom hole pressure without friction becomes larger than the bottom hole pressure with friction. The reason for this can be explained by observing Figures 9, 10, 11 and 12, which represent respectively: closed chamber pressures for both cases, hydrostatic fluid pressure drops for both cases, frictional pressure drop for the basecase with friction, and oil flowrates for both cases.

According to these figures, during the first 20 seconds of the test, the most important factor in the bottom hole pressure response is given by the elevation pressure as well as the friction pressure, which is proportional to the fluid level. During these 20 seconds both pressure drops are increasing. But, because of the friction effects, the fluid level rise is delayed in the case when friction is considered (Fig. 10). The chamber pressure, when no frictional effects are considered, starts its abrupt rising earlier than in the friction case (Fig. 9). After 20 seconds, the frictional pressure drop starts diminishing rapidly (Fig. 11) due to the decreasing oil flowrate (Fig. 12); the hydrostatic fluid pressure drop is practically constant and equal for both cases; and the chamber pressure is higher in the case without friction than with friction. All effects combined result in frictionless late time bottom hole pressures higher than the late time bottom hole pressures with friction.

Figures 13 and 14 represent the log-log early and late time responses for the basecase with and without friction. The log-log early and late time responses are represented as functions of the dimensionless variables defined in section 3 of this study. The early time response is significantly affected by the presence of wellbore friction, while the late time responses are very similar for both cases as can be observed in Figure 14.

TABLE 1. BASECASE PARAMETERS

Parameter	Value
Chamber Diameter	2.441 inches
Roughness	0.00060 inches
Relative Roughness	0.00025
Total Chamber Length	1000 feet
Initial Fluid Height	0 feet
Initial Chamber Pressure	30 psig
Chamber Gas Gravity	0.65 (to air)
Initial Reservoir Pressure	5000 psig
Reservoir Temperature	175 F
Produced Fluid Specific Gravity	25 API
Produced Fluid viscosity	1.25 cp
Porosity	27 %
Reservoir Permeability	100 md
Skin	0
Well Diameter	10 inches
Formation Total Compressibility	10×10^{-6} psi⁻¹
Formation Thickness	25 feet
Total Test Time	100 seconds

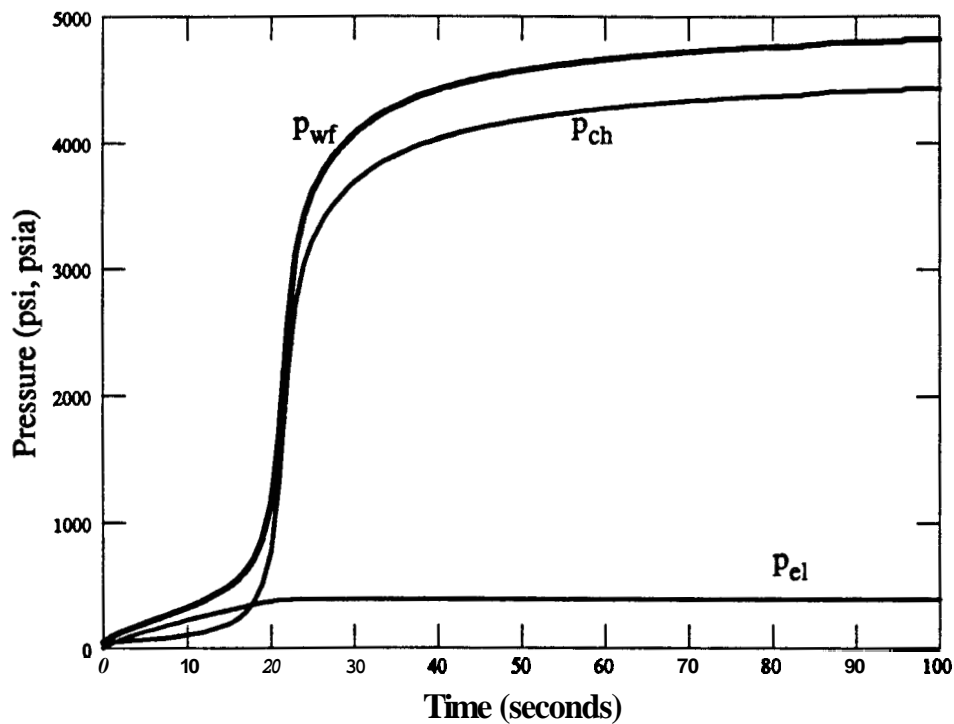


Figure 6: Basecase Without Friction

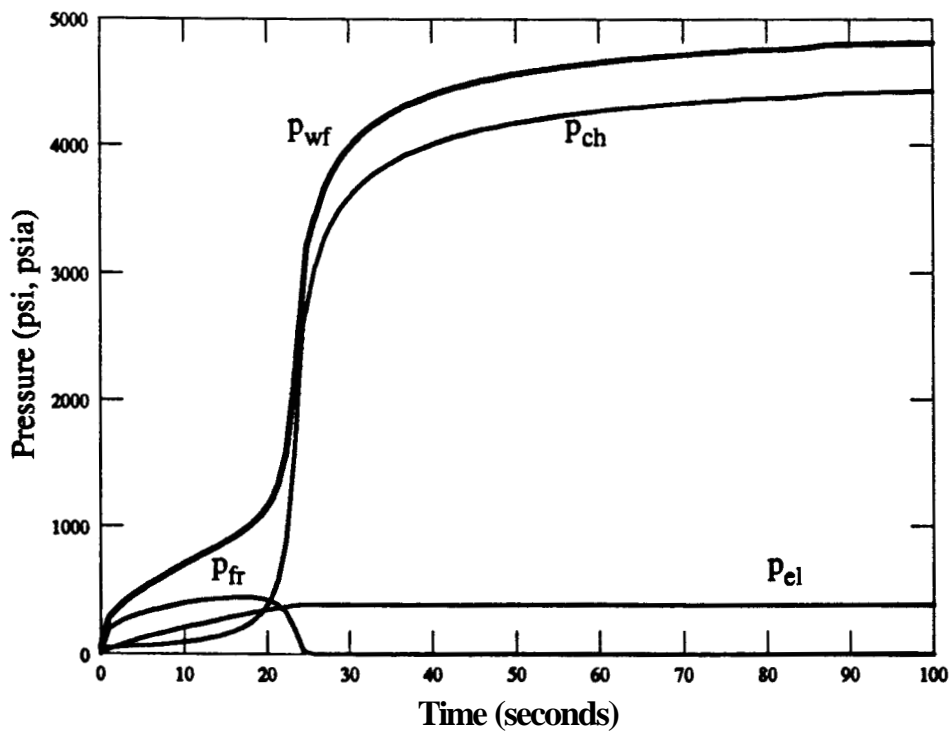


Figure 7: Basecase With Friction

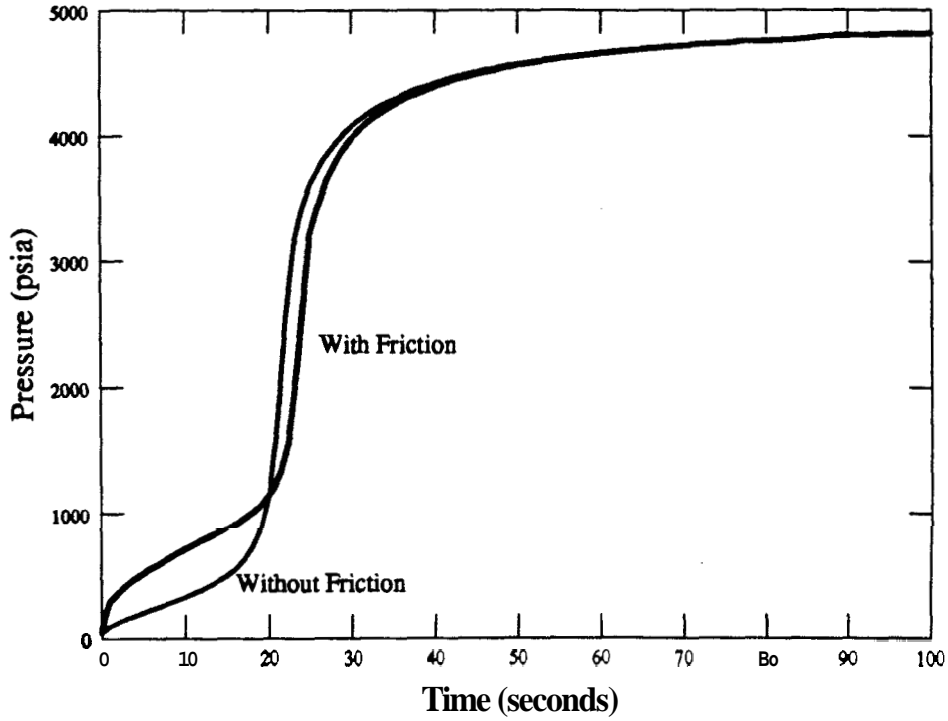


Figure 8: Bottom Hole Pressure for Basecase With and Without Friction

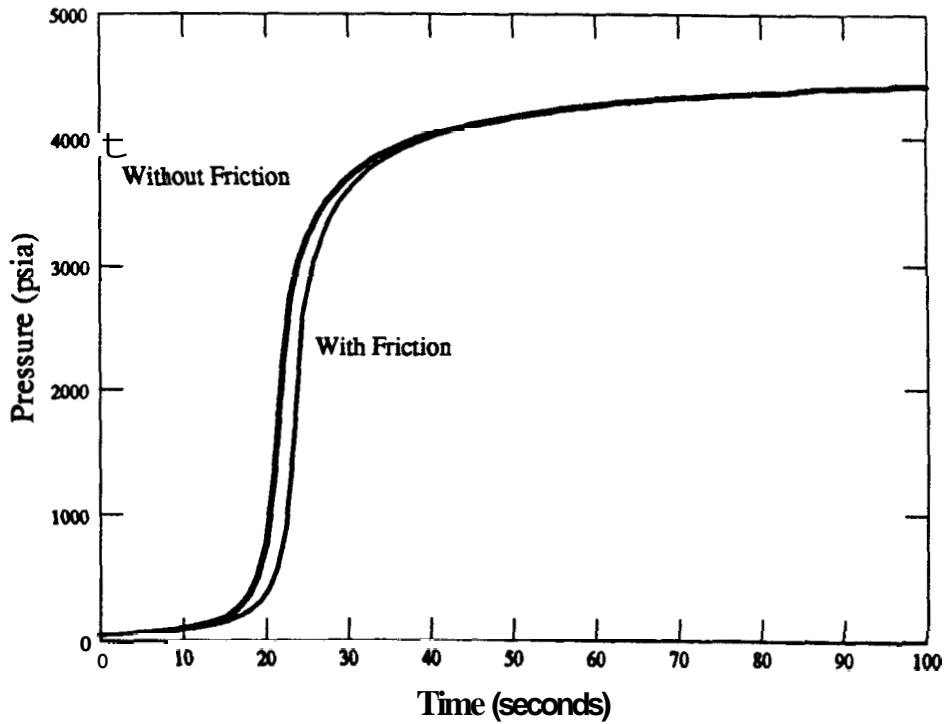


Figure 9: Chamber Pressure for Basecase With and Without Friction

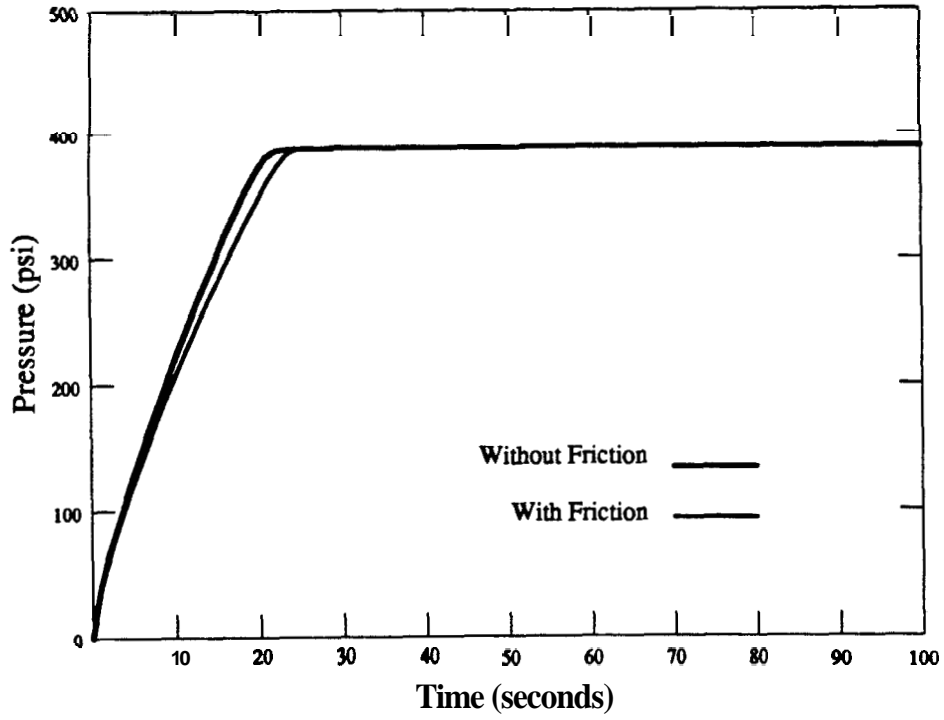


Figure 10: Elevation Pressure for Basecase With and Without Friction

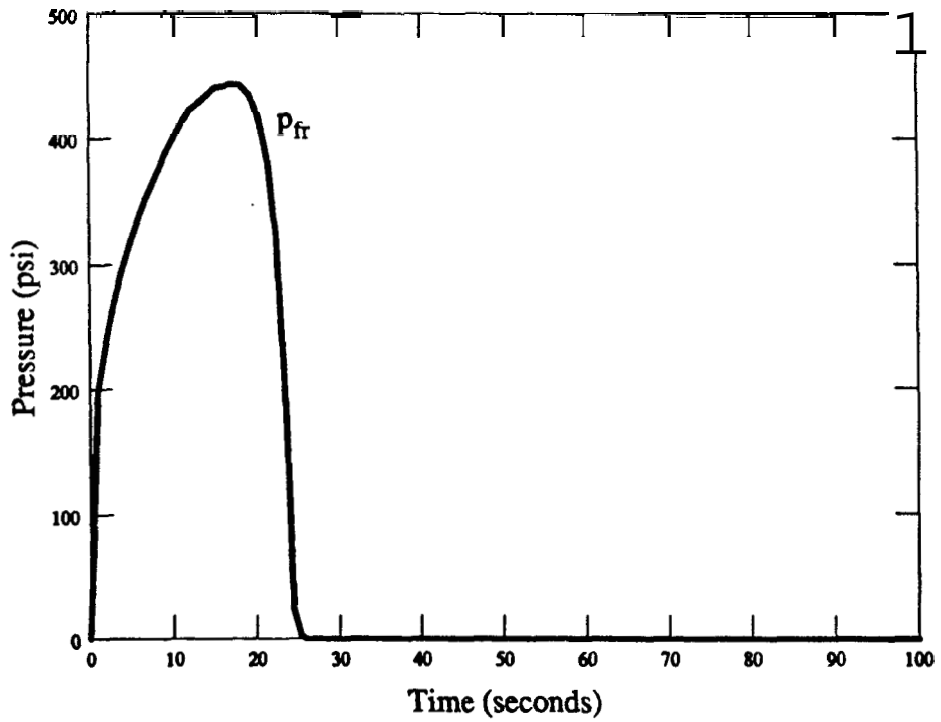


Figure 11: Frictional Pressure Drop for Basecase

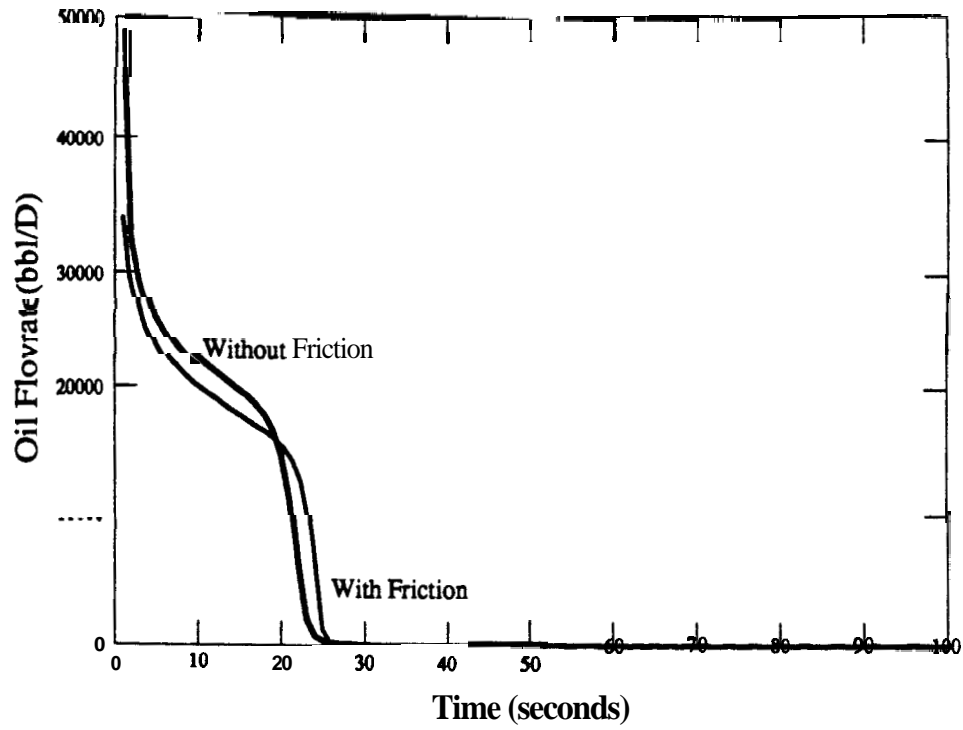


Figure 12: Oil Flowrate for Basecase With and Without Friction

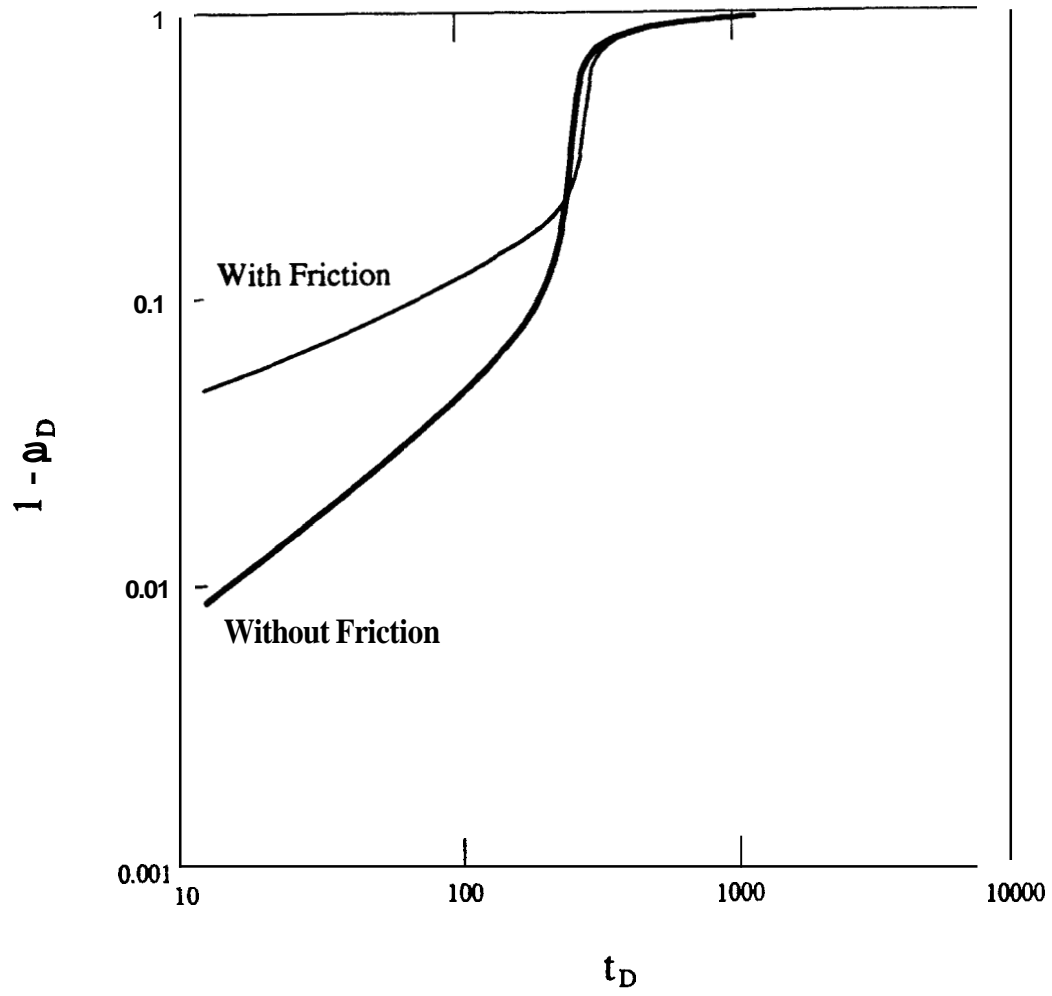


Figure 13: Early Time Plot for Basecase With and Without Friction

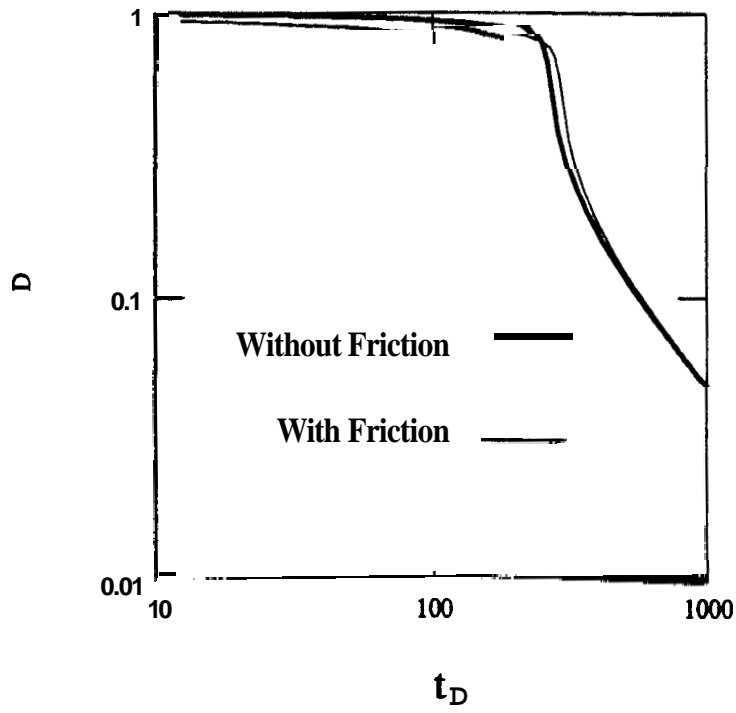


Figure 14: Late Time Plot for Basecase With and Without Friction

5. SENSITIVITY STUDY

In this section we present a sensitivity study of various tool and reservoir parameters of the closed chamber test, including frictional effects.

5.1. Effect of Wellbore Skin

Skin effect values of 0, 2 and 5 were considered in the sensitivity study. Figure 15 presents the bottom hole pressure response, including Friction effects, for the skin values considered in the analysis. Since the presence of wellbore skin reduces the sandface flowrate into the wellbore, the rapid pressure rise during chamber compression is delayed. Yet, the final fluid level and the late time responses are **similar**. The frictional pressure drops for these skin values are illustrated in Figure 16. According to this figure, the frictional pressure drop is smaller but lasts longer as the skin value increases. The reason for **this** is explained in Figure 17, that represents the oil flowrate **for** the skins studied. For higher skins the oil flowrate is smaller and decreases slower than for lower skins. In other words, because the cross sectional area of the pipe remains constant, and the initial fluid conditions are identical the fluid rises to the same level in all cases.

Log-log early and late time plots are presented in Figures 18 and 19. Like in the cases studied by **Simmons**, the late time format gives the largest resolution to skin effect. The early time response in the presence of wellbore skin differs significantly **from** the early time response **without** wellbore skin **as** shown by **Sageev (1986)**. In the early time log-log format the **slope** of the pressure response without wellbore skin **is 1/2**, denoting transient linear flow. The early time response **with** wellbore skin has a unit slope, representing constant flow rate.

The bottom hole pressure responses, with and without friction, for skin values of 0, 2 and 5, are presented in Figures 8, 20 and 21 respectively. Because the frictional pressure drop decreases **as** the skin value **increases**, the difference between both curves becomes less significant for larger **skins**.

By observing the dimensionless plots of the pressure response, with and without friction, for the different skins analyzed (Figs. 13, 14, 22, 23, 24 and 25), we conclude that the late time plot matches better both responses. Moreover, for larger skins the difference between the curves is insignificant.

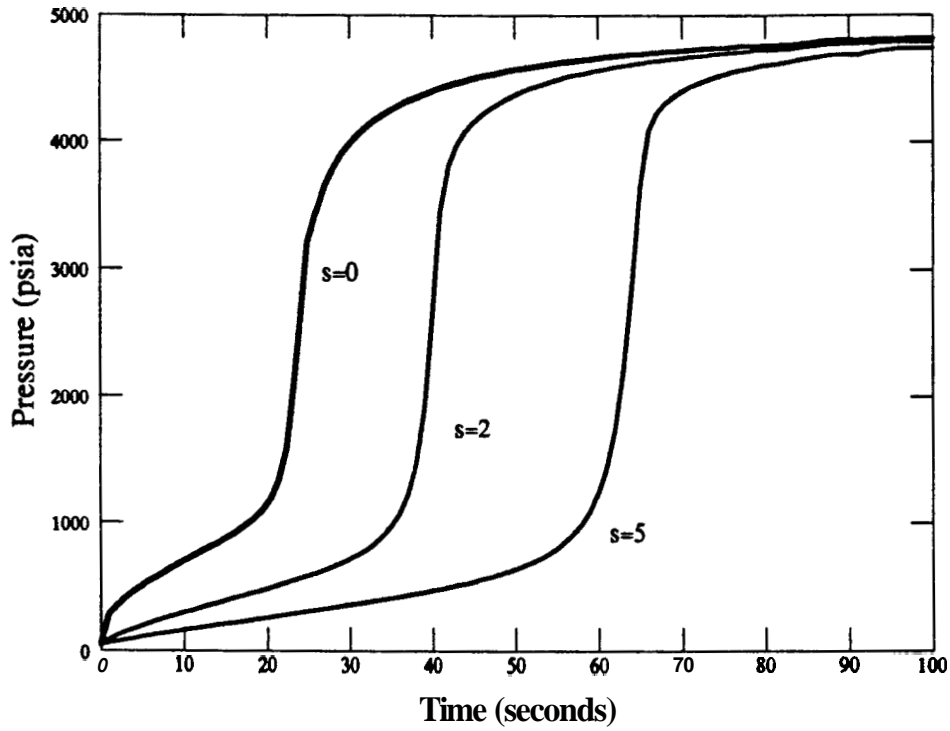


Figure 15: Bottom Hole Pressure for Different Skins

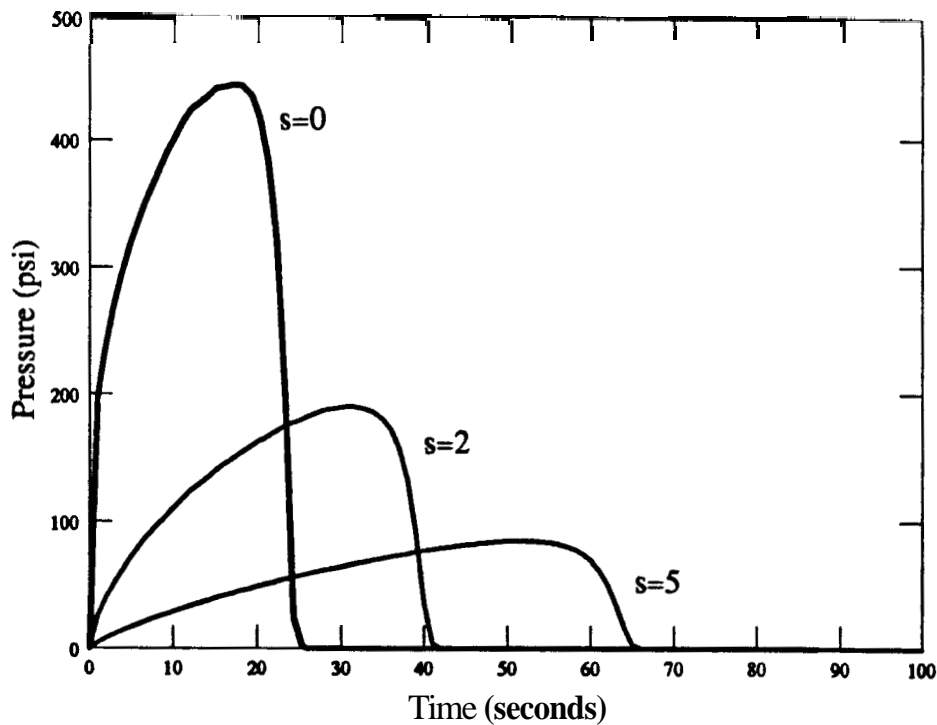


Figure 16: Frictional Pressure Drop for Different Skins

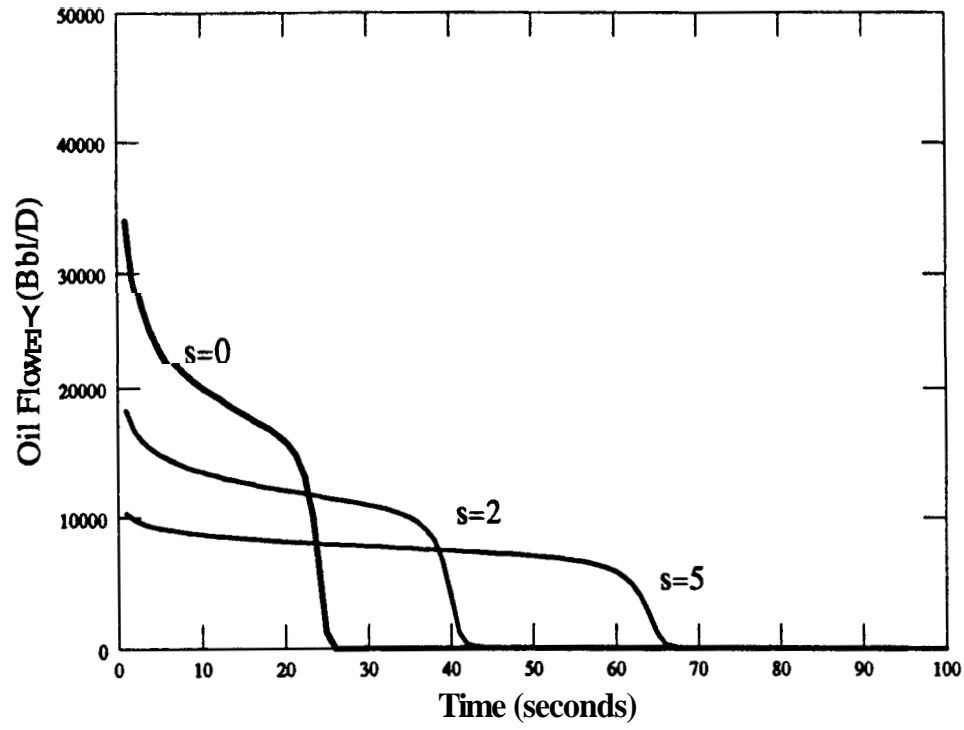


Figure 17: Oil Flowrate for Different Skins

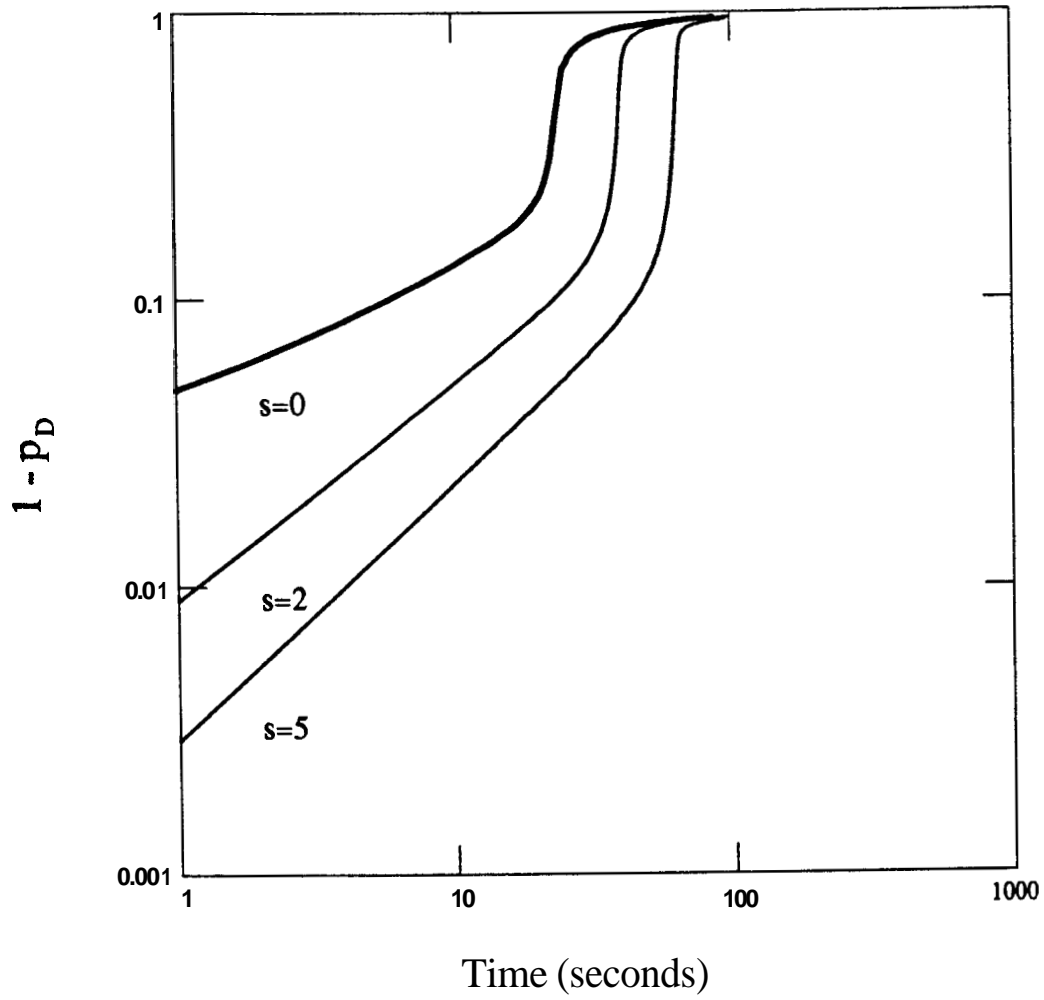


Figure 18: ~~Early~~ Time Plot for Different Skins

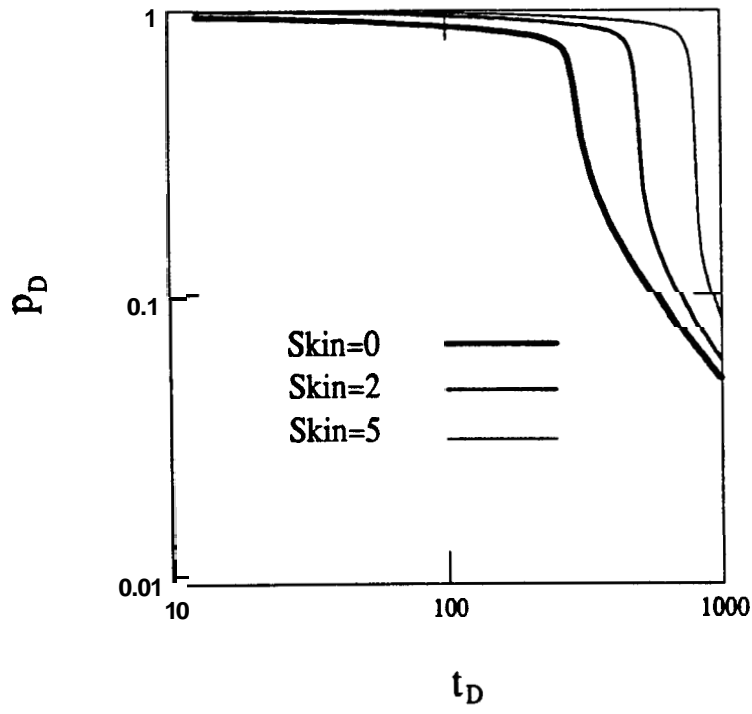


Figure 19: Late Time Plot for Different Skins

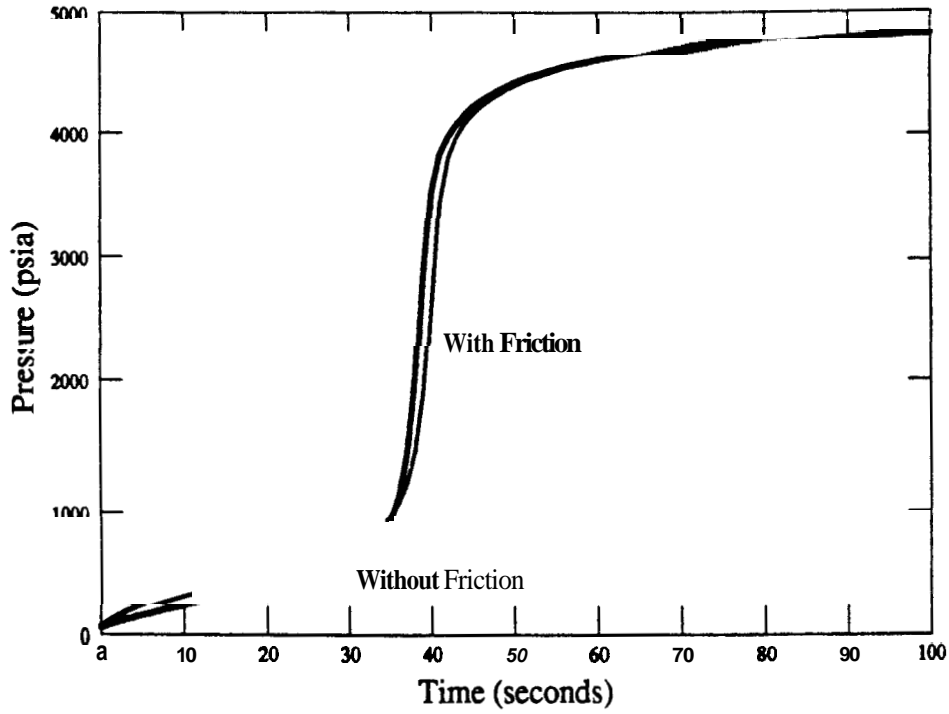


Figure 20: Bottom Hole Pressure for Skin=2 With and Without Friction

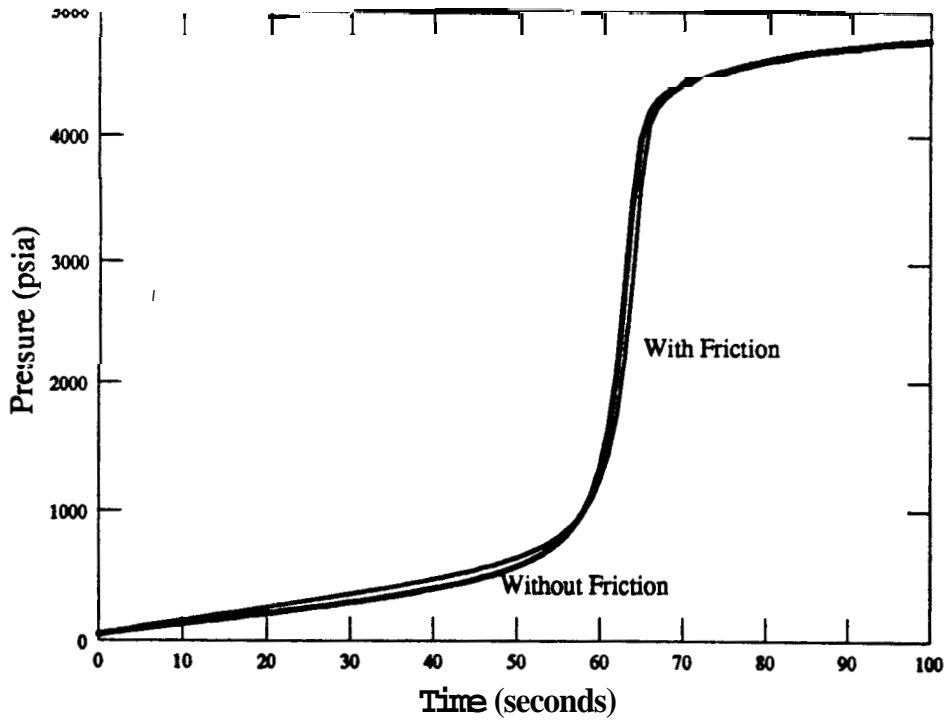


Figure 21: Bottom Hole Pressure for Skin=5 With and Without Friction

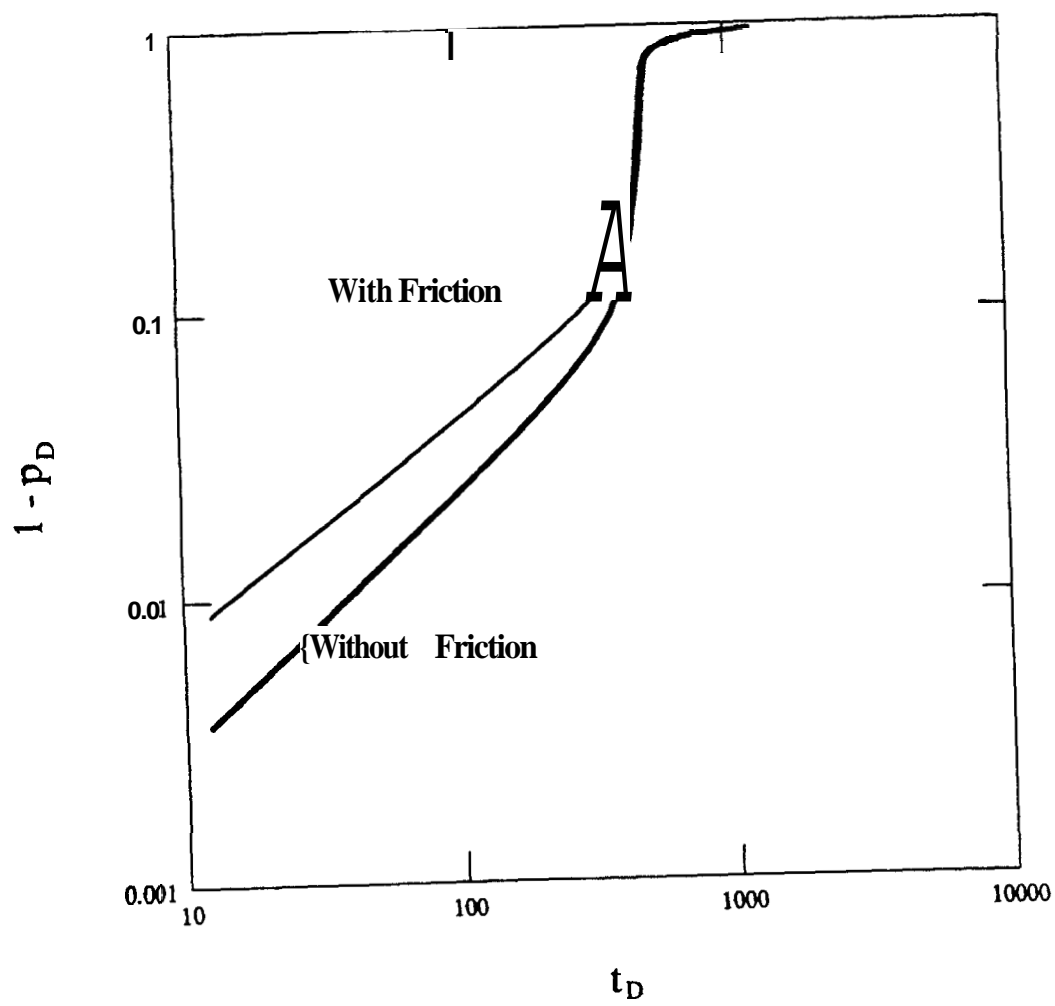


Figure 22: ~~Early Time~~ Plot for Skin-2 With and Without Friction

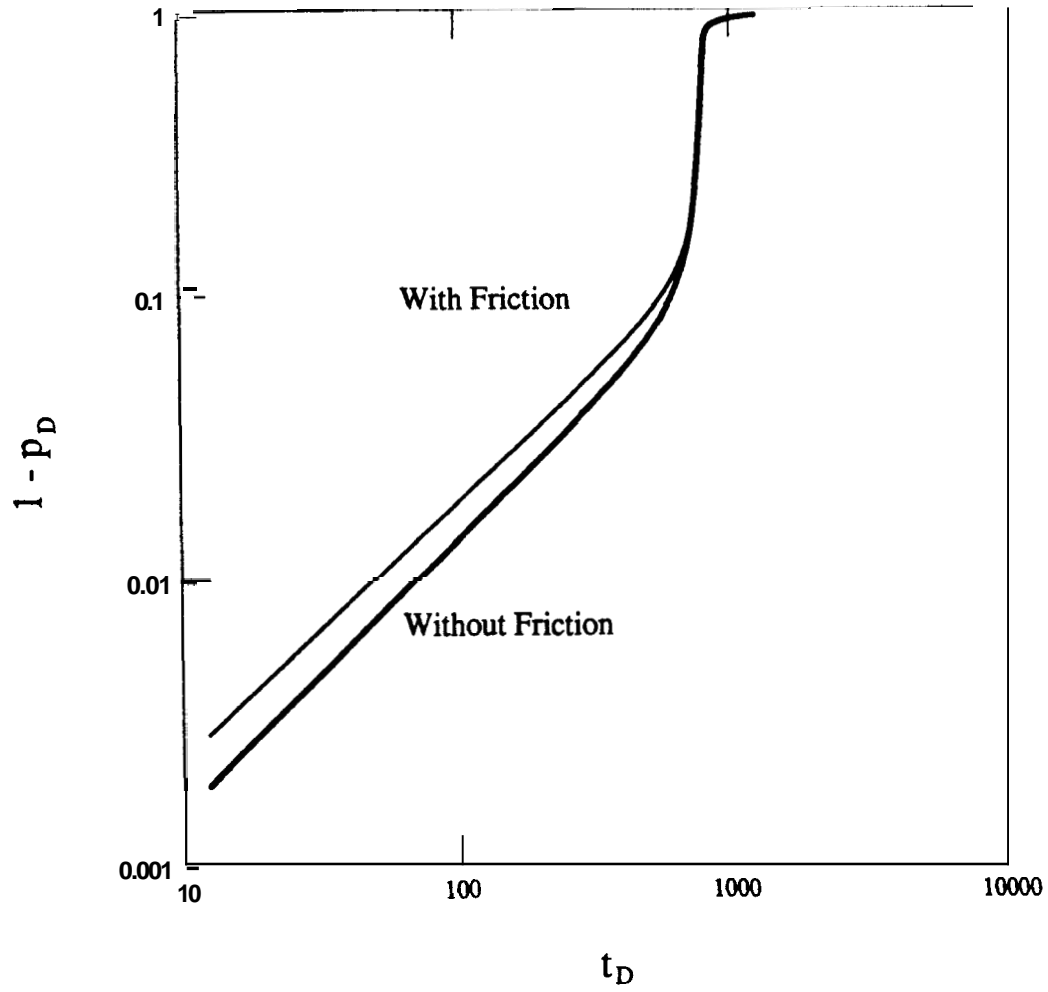


Figure 23: Early Time Plot for Skin=5 With and Without Friction

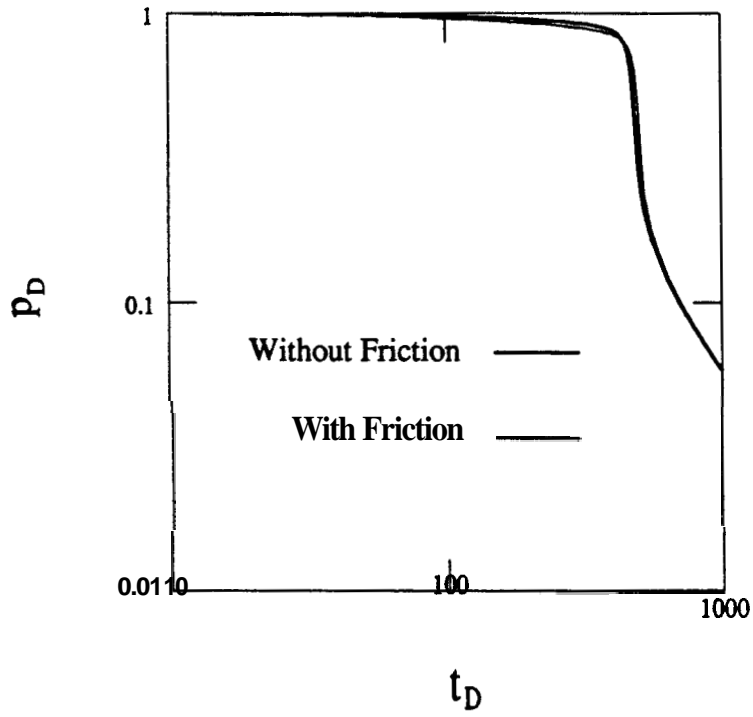


Figure 24: Late Time Plot for Skin=2 With and Without Friction

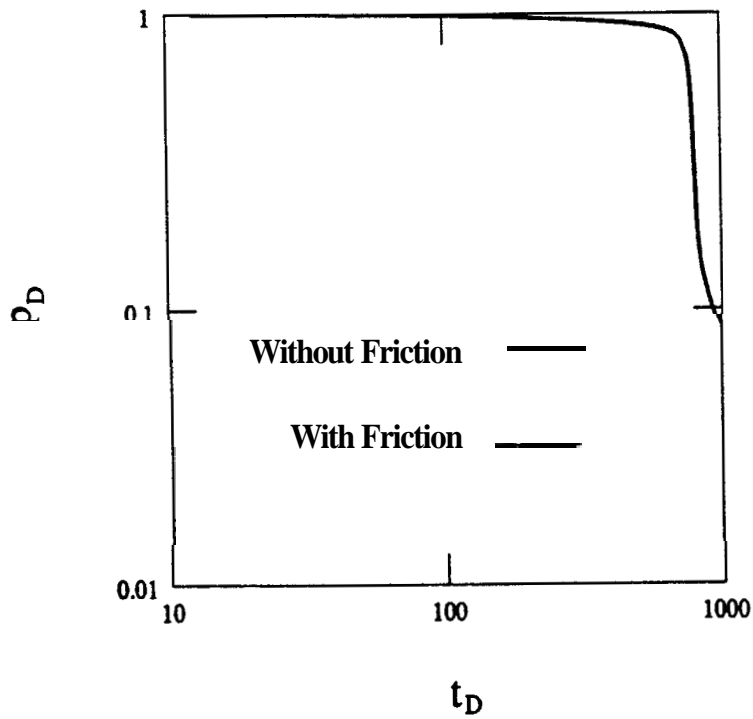


Figure 25: Late Time Plot for Skin=5 With and Without Friction

5.2. Effect of Initial Reservoir Pressure

The values for initial reservoir pressure considered in the analysis were **3000** and 5000 psig, where the last one corresponds to the basecase.

Figure 26 shows the influence of the initial reservoir pressure on the bottom hole pressure when considering wellbore frictional effects. **As** expected, the bottom hole pressure response tends to the initial static reservoir pressure. Like in the cases presented by *Simmons*, the period of rapid pressure rise due to gas compression occurs earlier for higher pressure formations.

As can be observed in Figure 27, the frictional pressure drop is smaller and lasts longer **as** the initial reservoir pressure decreases. The reason for this is that the oil flowrate for higher pressure formations is larger because the greater initial pressure differential at the sandface (Figure 28). However, since the final volume of oil produced is about the same, (chamber **gas** is compressed **to** different pressures), the areas under the flowrate curves (Figure 28) are about the same.

Log-log early and late time plots for different initial reservoir pressures are presented in Figures 29 and 30. Again, since skin is not present, the early time response is similar to the slug test response with a slope of $1/2$. The late time log-log pressure response approaches the unit slope of the line source slug test response presented by *Ferris and Knowles* (1954).

Figure 31 illustrates the bottom hole pressure response, with and without friction, for the case when **the** initial reservoir pressure is 3000 psig. Comparing this figure to the figure corresponding to the basecase (Figure 8), it *can* be inferred that the relative effect of friction in lower initial reservoir pressure **formations** is smaller than in higher pressure formations.

Figures 32 and 33 present the early and late time plots **for an** initial reservoir pressure of **3000** psig, with and without friction and without wellbore skin. For smaller initial reservoir pressures the **late** time portion collapses better because the frictional effects in these cases are smaller.

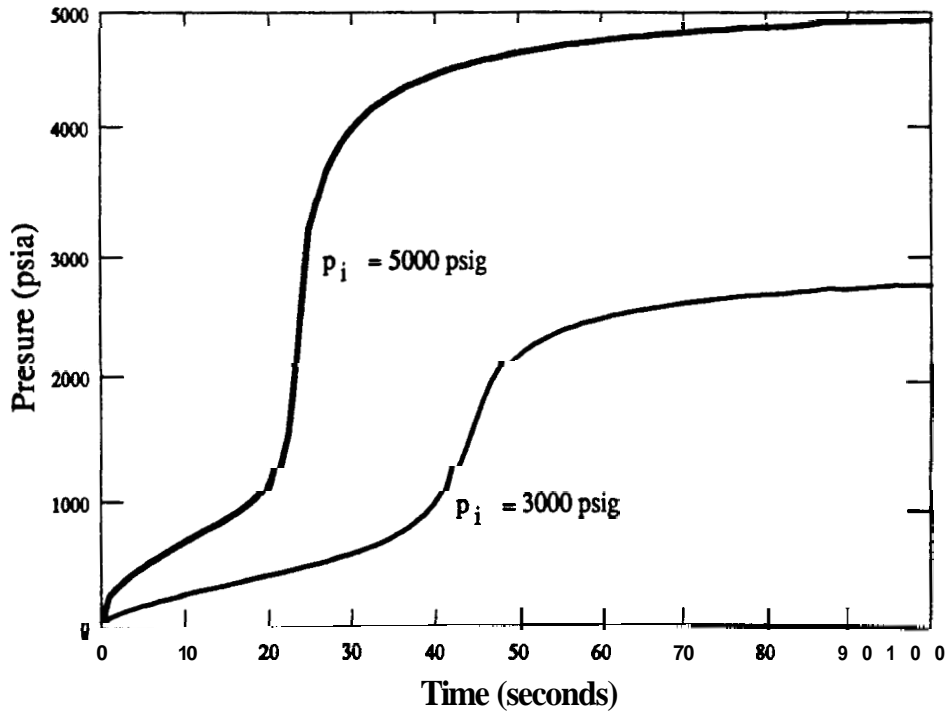


Figure 26: Bottom Hole Pressure for Different Initial Reservoir Pressures

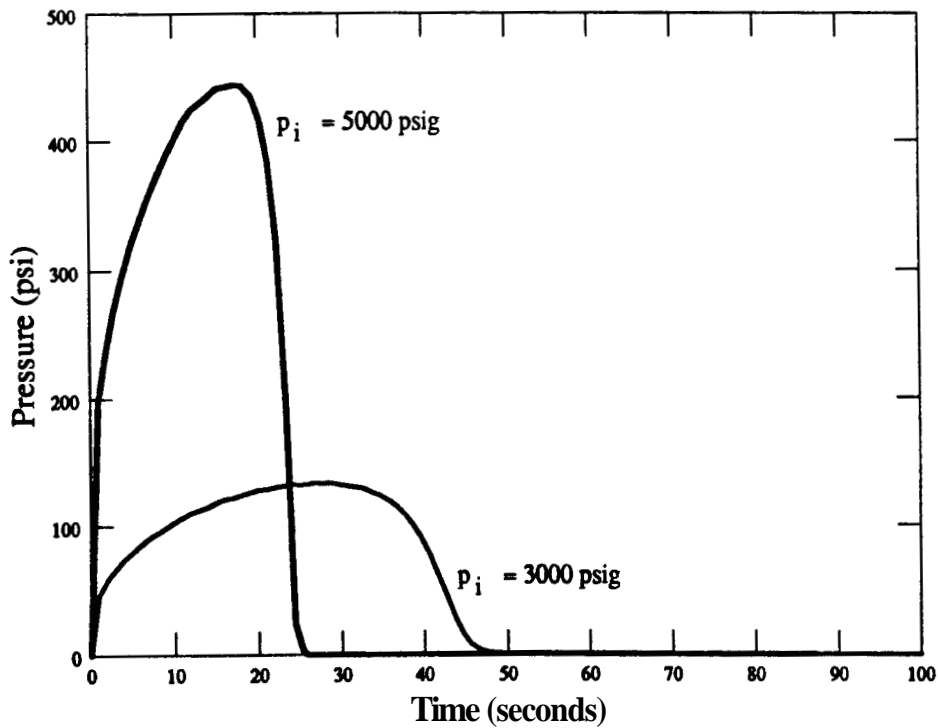


Figure 27: Frictional Pressure Drop for Different Initial Reservoir Pressures

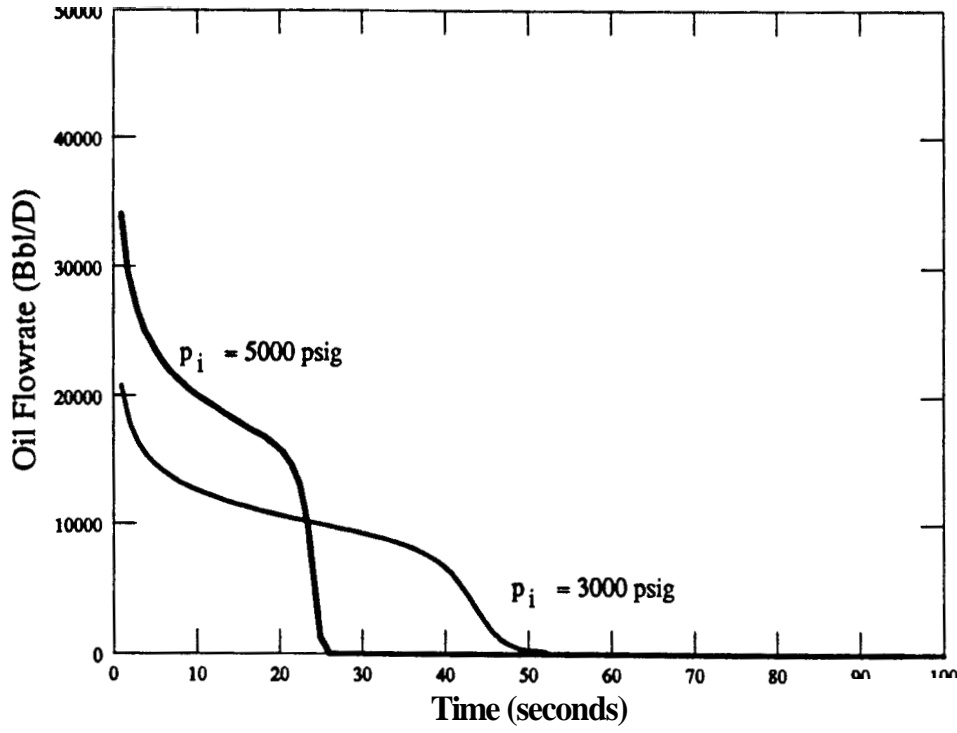


Figure 28: Oil Flowrate for Different Initial Reservoir Pressures

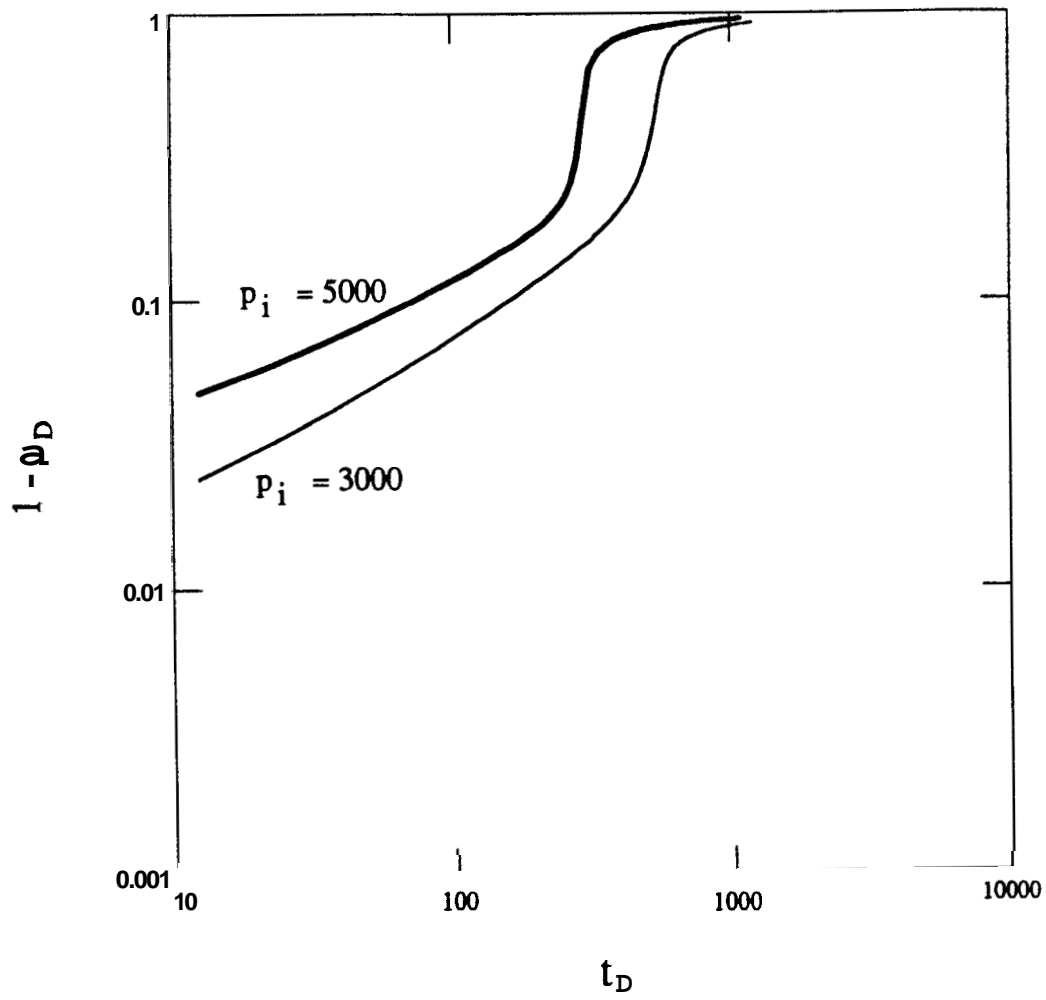


Figure 29: ~~Early~~ Time Plot for Different Initial Reservoir Pressures

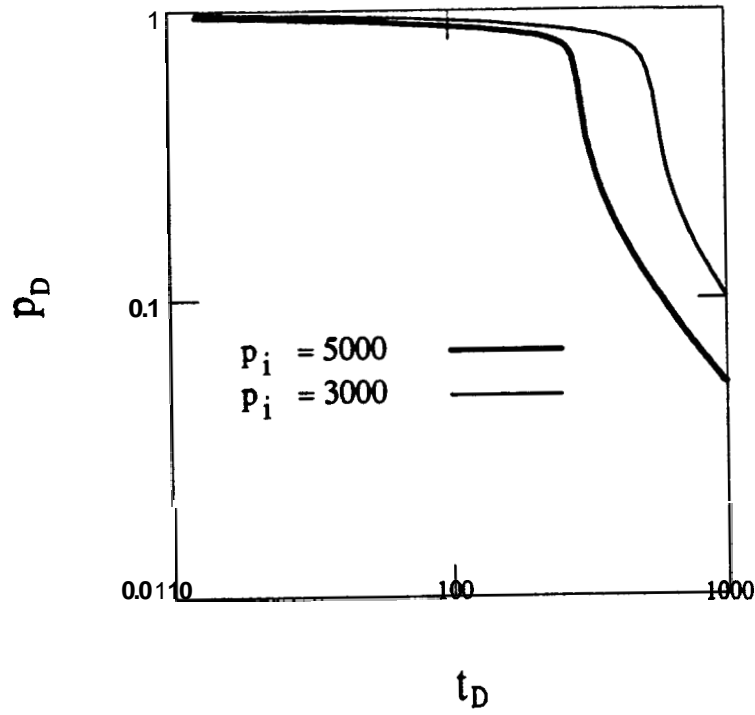


Figure 30: Late Time Plot for Different Initial Reservoir Pressures

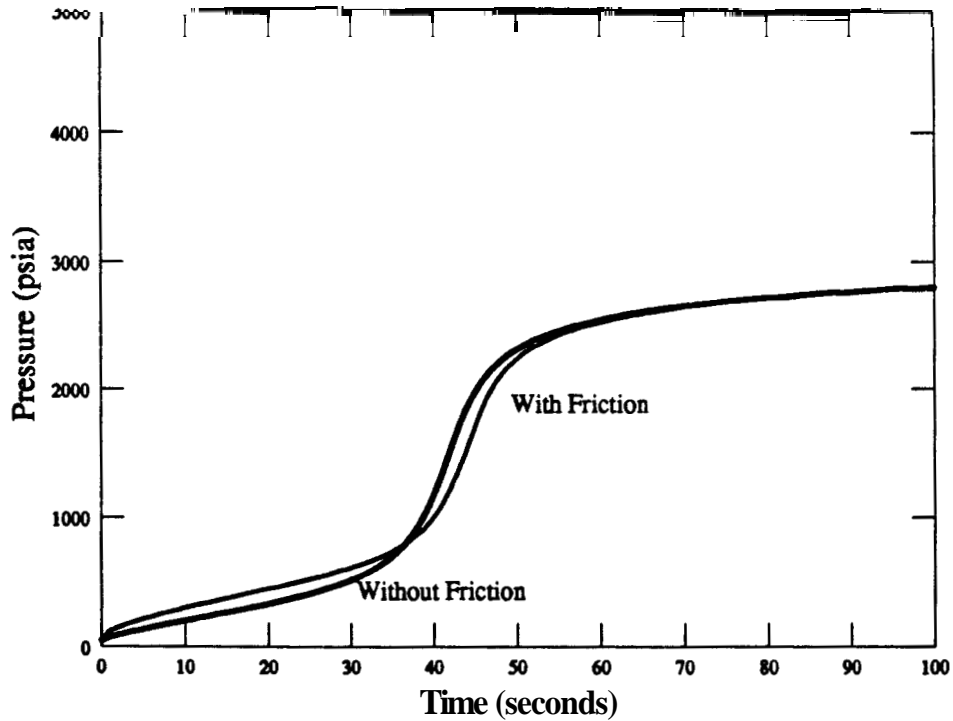


Figure 31: Bottom Hole Pressure for $p_i = 3000$ psig with and without friction

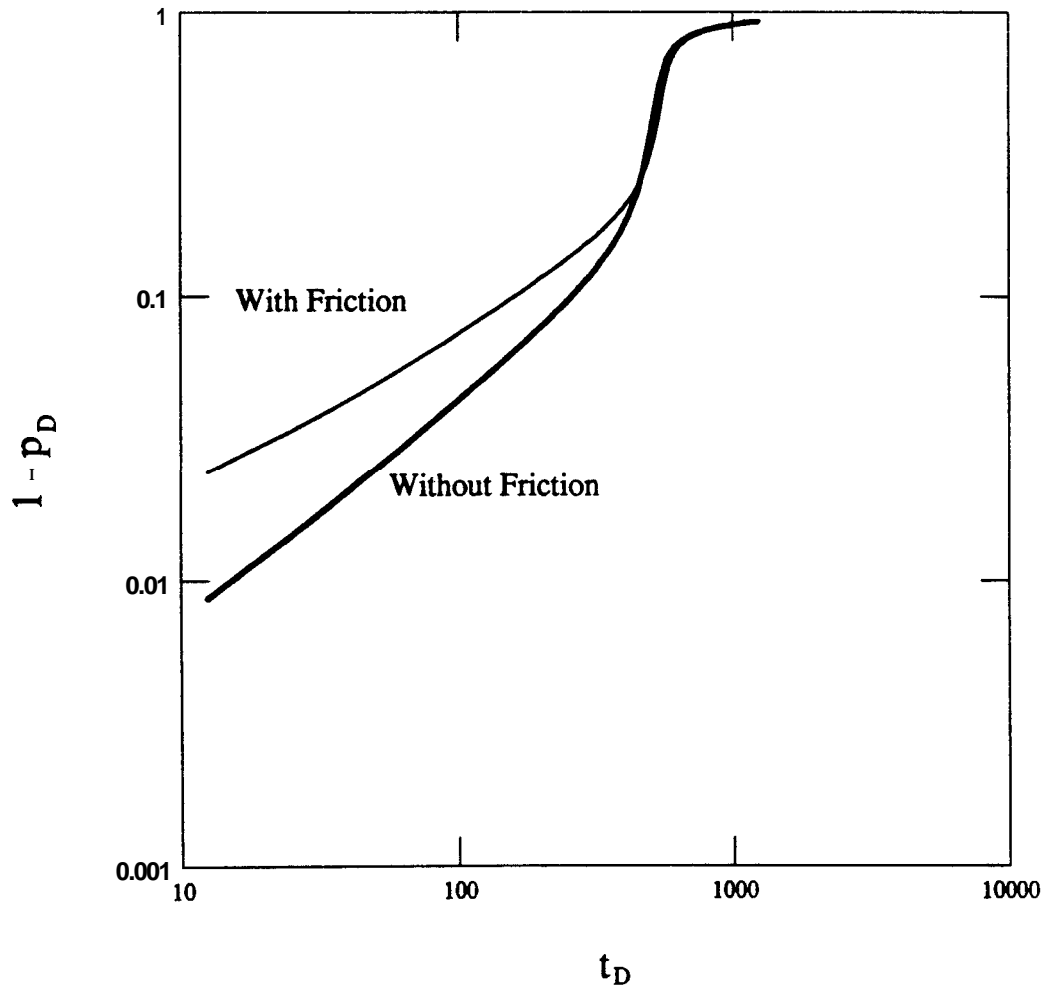


Figure 32: Early Time Plot for $p_i=3000$ psig with and without friction

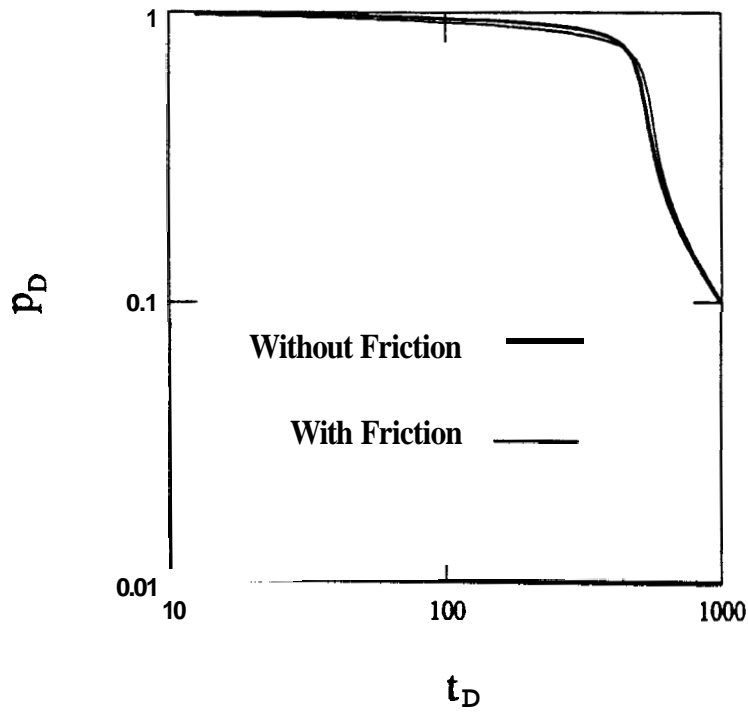


Figure 33: Late Time Plot for $p_i=3000$ psig with and without friction

53. Effect of Chamber Diameter

The closed chamber pressure response was studied for two chamber diameters, **2.441** and **4.0** inches. The closed chamber pressure response when considering frictional effects in the wellbore is closely related to the chamber diameter because the frictional head loss is inversely proportional to D^5 .

Figure **34** presents the bottom hole pressure for the two cases studied. **As** the tubing diameter increases, the rapid chamber compression is delayed. The frictional pressure drops for these cases are represented in Figure **35**. **As** the chamber diameter is increased the friction pressure losses become less important in the behavior of the total pressure response. For example, according to Figure **36**, for a chamber diameter of **4.0** inches, the friction pressure loss is practically negligible though it lasts longer, and both pressure responses, with friction and without it, are practically identical.

The oil flowrate for both cases of Figure **34** are shown in Figure **37**. As expected, the area beneath the curve for a chamber diameter of **4.0** inches is larger than the area beneath the curve corresponding to a chamber diameter of **2.441** inches, since wellbore volume is larger. Like in the no-friction cases presented by *Simmons*, there is a dimensionless time shift to the right on the early and late time log-log pressure responses due to larger chamber diameters (Figures **38** and **39**).

Early and late time plots for the case corresponding to a chamber diameter of 4.0 inches can be observed in Figures **40** and **41**. Again, for a larger chamber diameter, because the frictional pressure drop is smaller, the late time log-log responses are practically identical. The early time **log-log** responses are slightly different during the "slug test" response. However, during the rapid pressure rise and thereafter the responses are practically identical

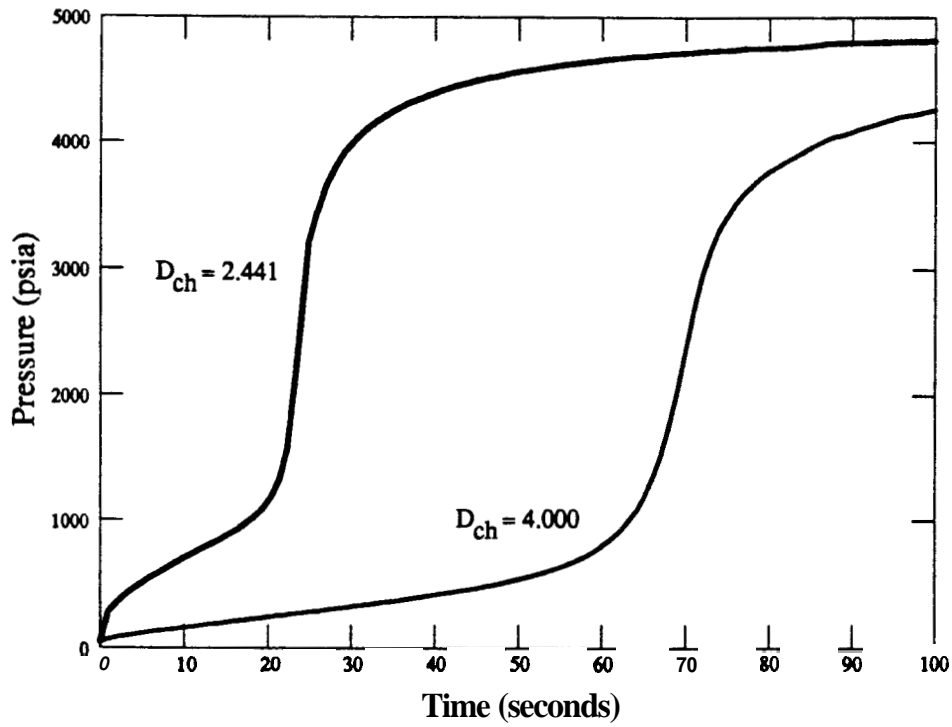


Figure 34: Bottom Hole Pressure for Different Chamber Diameters

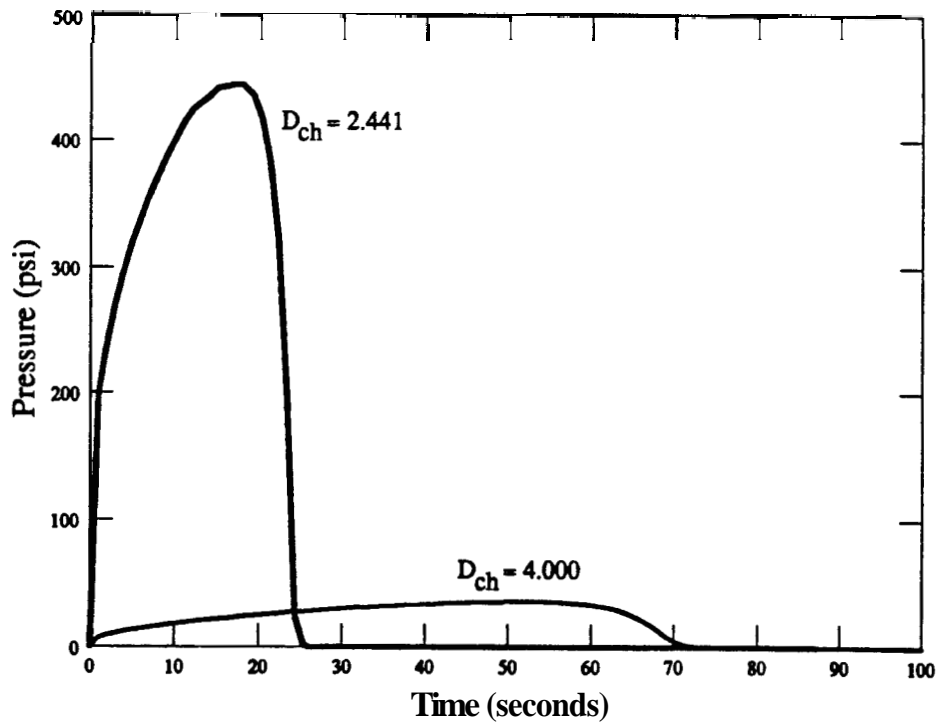


Figure 35: Frictional Pressure Drop for Different Chamber Diameters

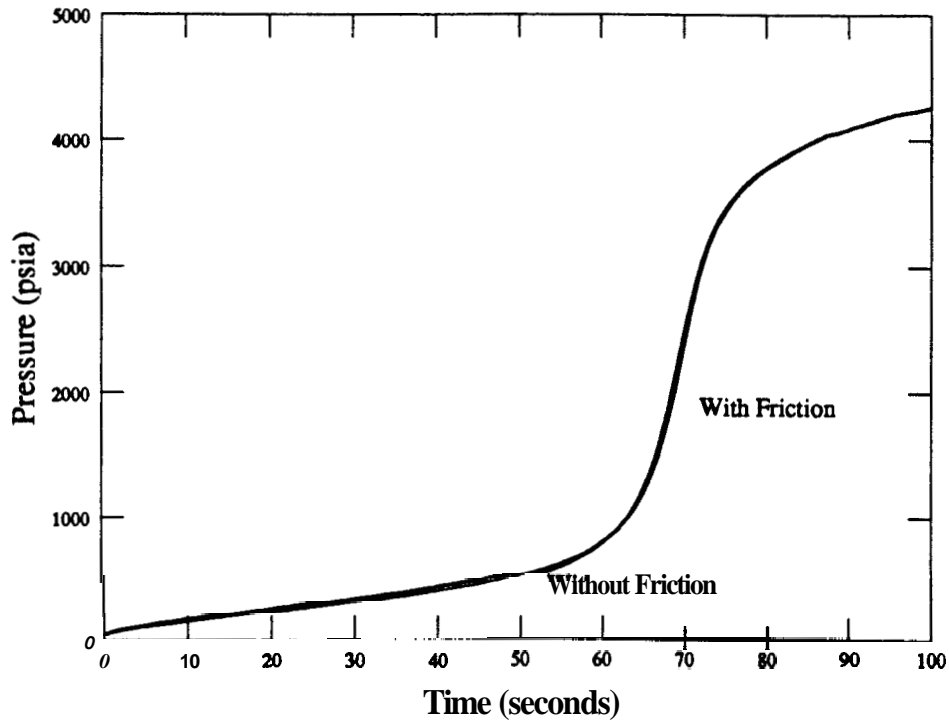


Figure 36: Bottom Hole Pressure for $D_{ch}=4.00$ inches With and Without Friction

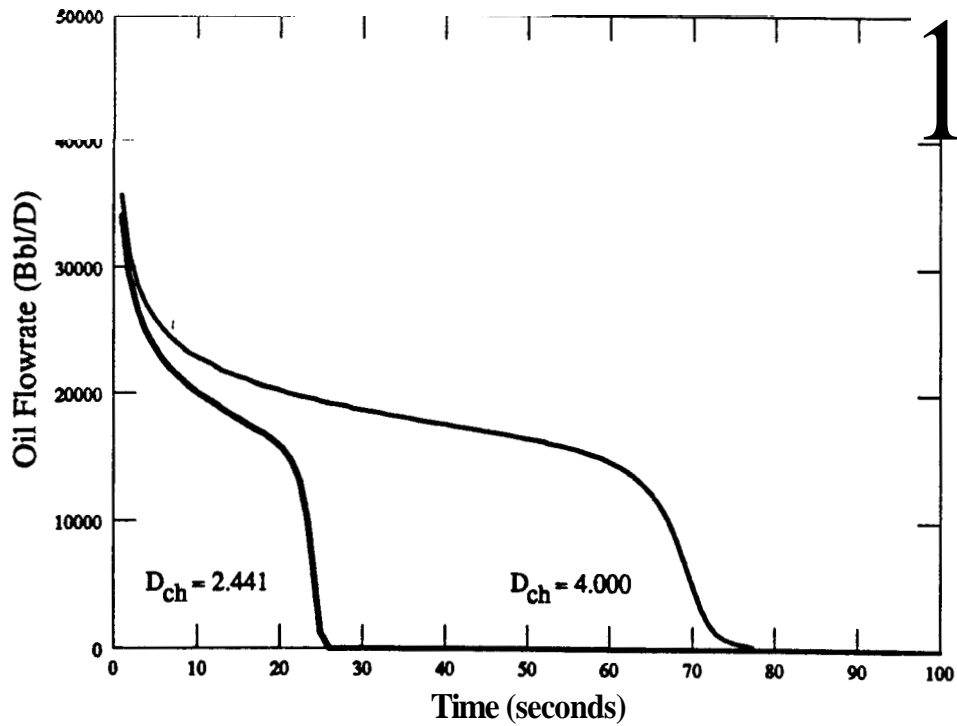


Figure 37: Oil Flowrate for Different Chamber Diameters

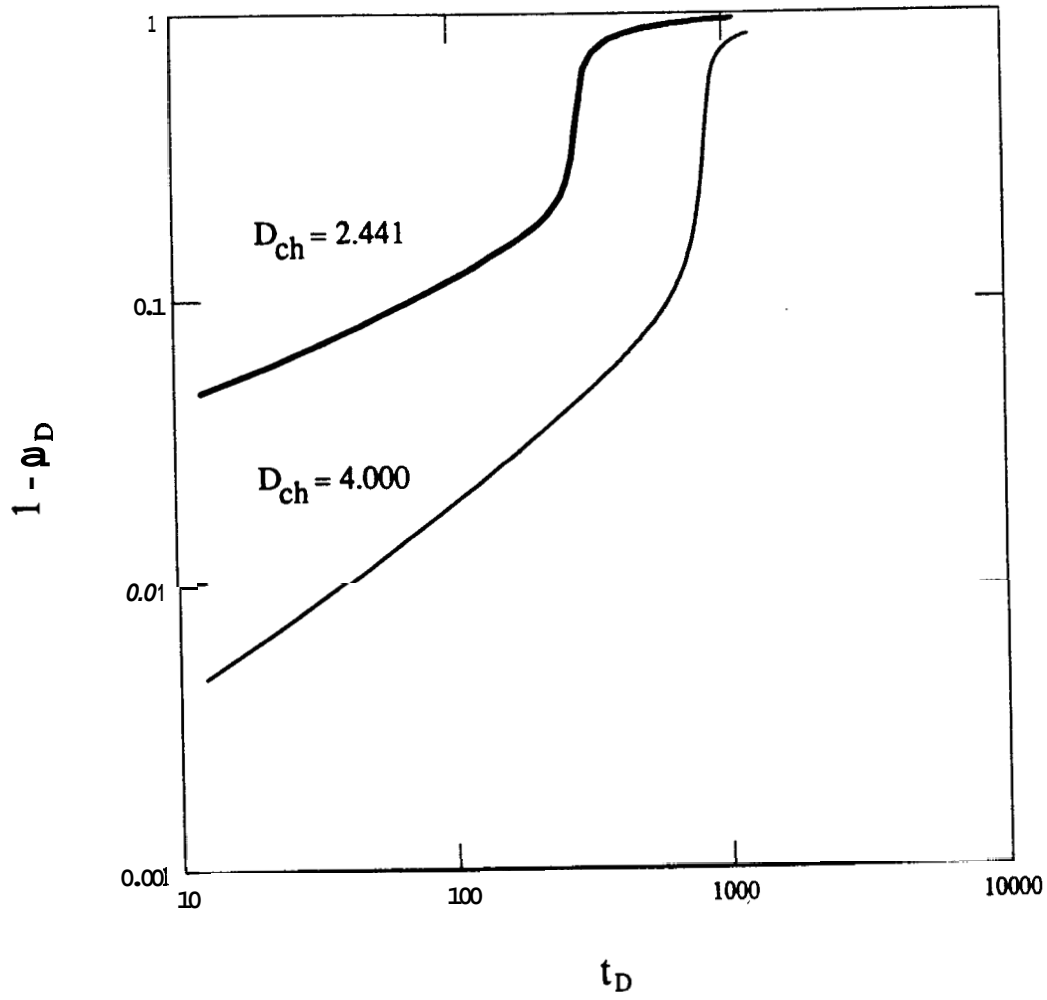


Figure 38: Early Time Plot for Different Chamber Diameters

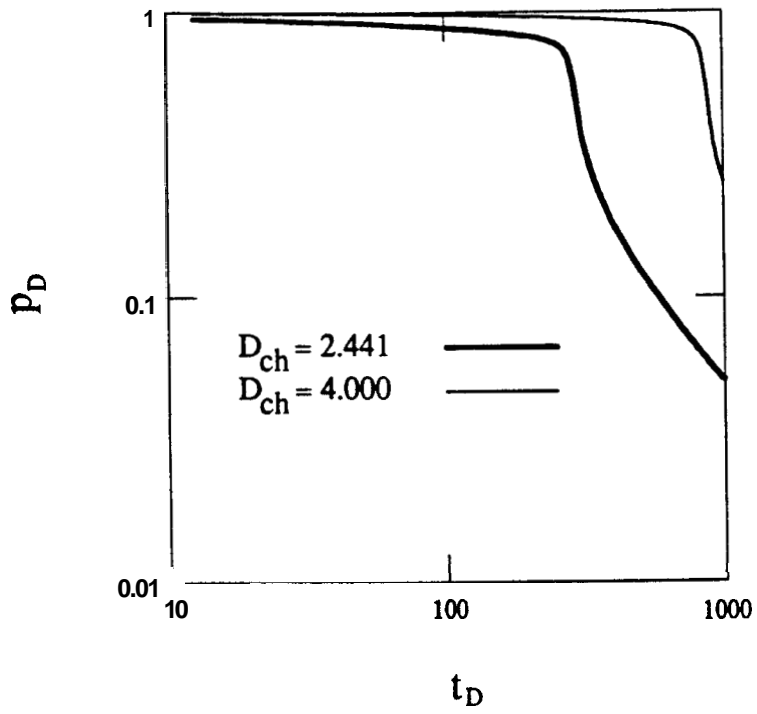


Figure 39: Late Time Plot for Different Chamber Diameters

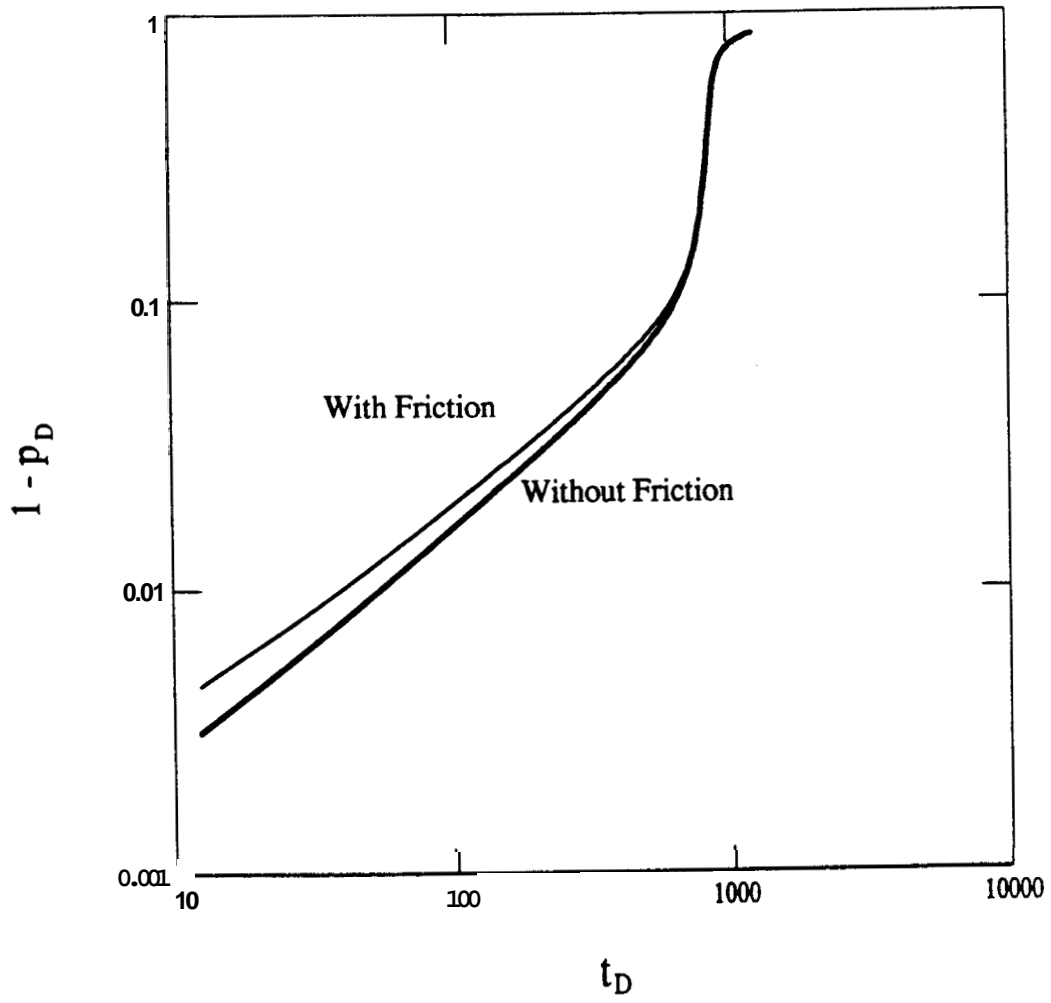


Figure 40: ~~Early~~ Time Plot for $D_{ch}=4.00$ inches With and Without Friction

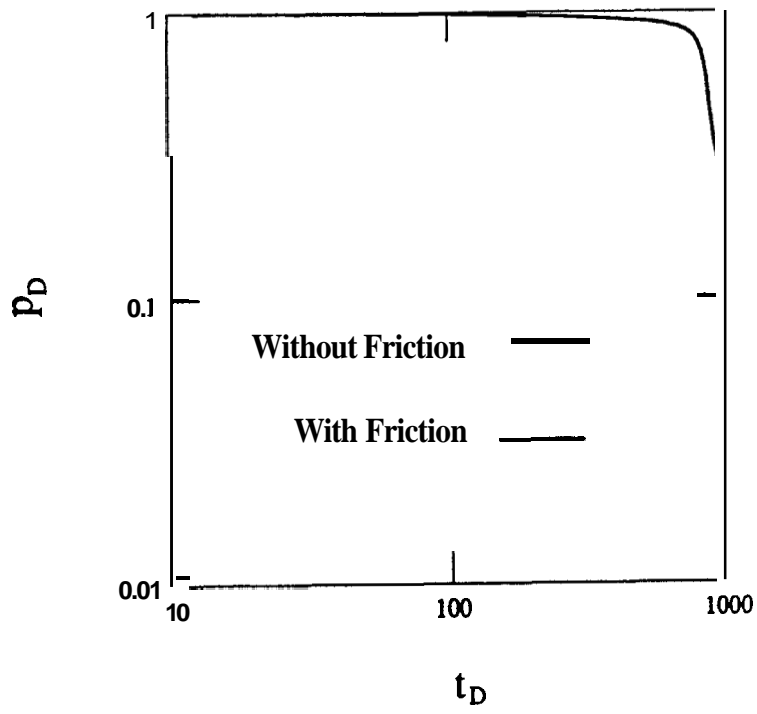


Figure 41: Late Time Plot for $D_{ch}=4.00$ inches With and Without Friction

54. Effect of Roughness

Because the Moody friction factor is a function of **the** relative roughness, e/D , we analyzed the influence of **this** parameter on the closed chamber pressure response. Two different values of the absolute roughness, e , were used in the sensitivity study.

A typical absolute roughness value selected for the basecase was 0.0006 inches. The corresponding relative roughness, for a chamber diameter of **2.441** inches, **is** 0.00025. To **perform** the analysis the another value considered for the absolute roughness was 0.00015 inches, that gives a relative roughness of 0.00006 for the same chamber diameter. It is important to notice that a skin value of **2** was used to generate the pressure response for the different relative roughness values.

Figures **42**, **43** and **44** present the results obtained. According to these figures, although the frictional pressure drop is lower for the smallest relative roughness, the bottom hole pressure response **is** not significantly altered. Also, the decreasing of the flowrate behaves in the same way for the two cases studied. The reason for this is that the flow regime in both cases lies in the transition zone where Moody friction factors do not vary much for different values of e/D .

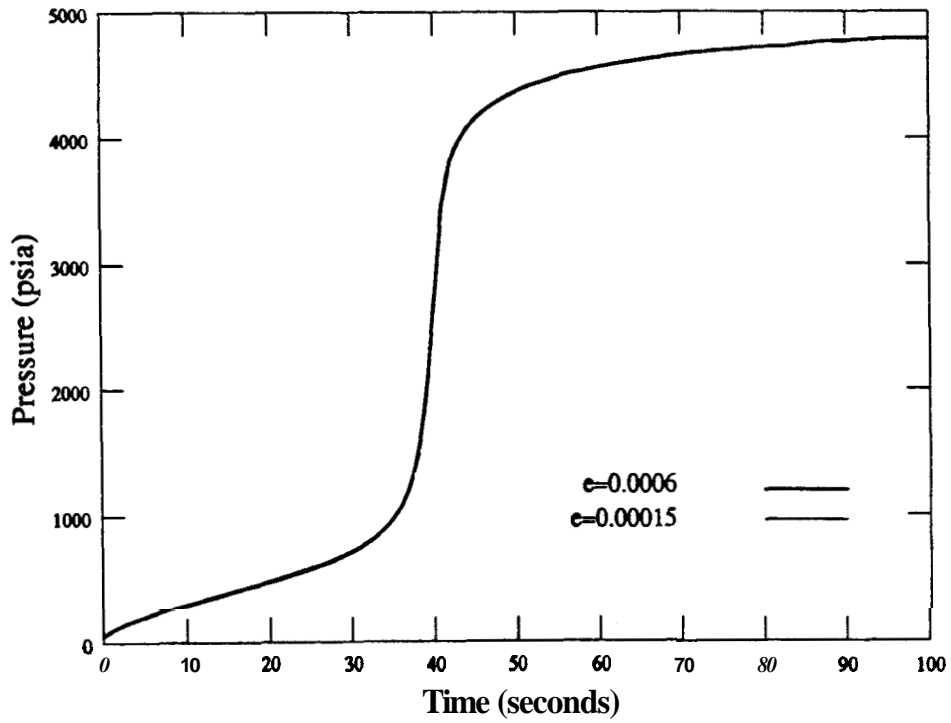


Figure 42: Bottom Hole Pressure for Different Roughness

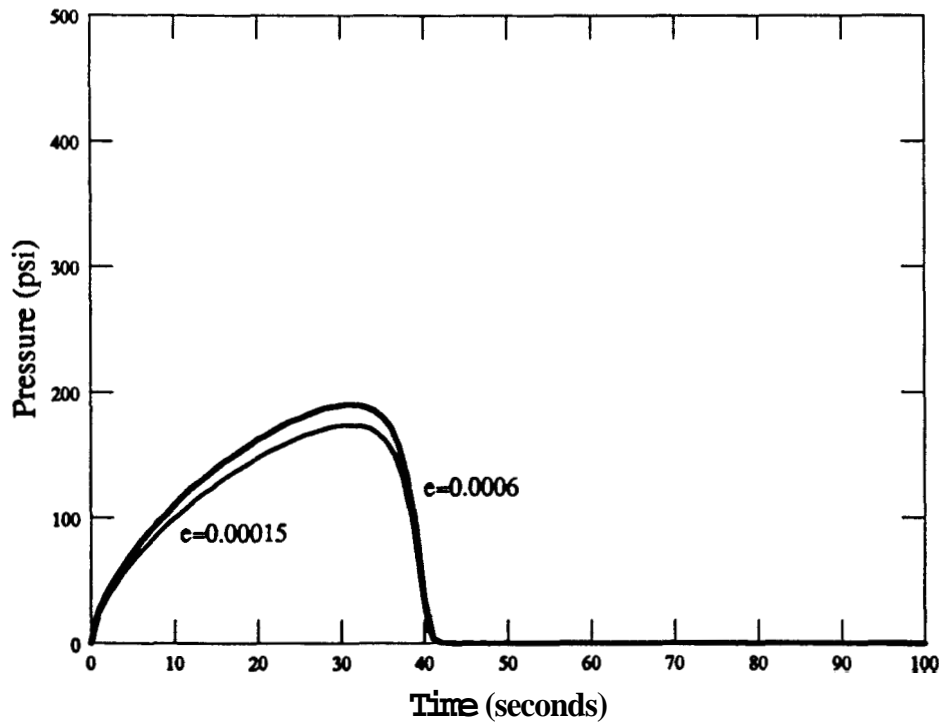


Figure 43: Frictional Pressure Drop for Different Roughness

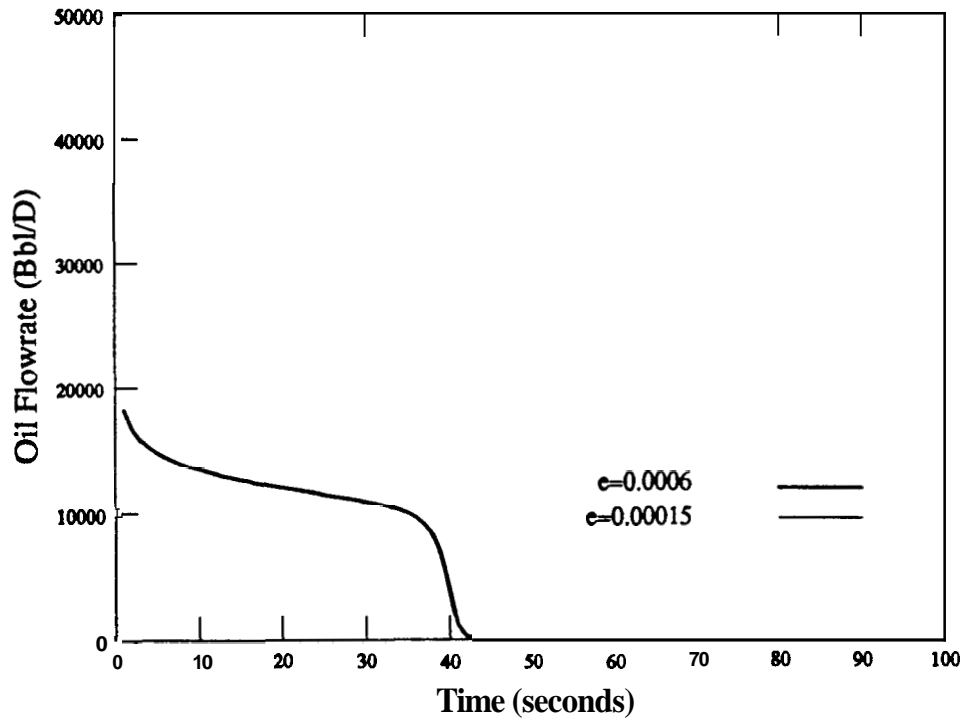


Figure 44: Oil Flowrate for Different Roughness

55. Effect of Initial Chamber Pressure

Two values of initial chamber pressure were considered: 0 and 30 psig (basecase). Again, the closed chamber pressure responses for these two values were generated for a skin value of 2. Figure 45 illustrates the bottom hole flowing pressure response for the two different values of initial chamber pressure. The frictional pressure drops for these are presented in Figure 46. Like in the no-friction cases studied by **Simmons**, larger initial chamber pressure values tend to smooth the pressure response. **Also**, as expected, the frictional pressure drops for these cases are smaller because less fluid rise is required, and the flowrates are smaller.

Early and late time dimensionless plots are presented in Figures 47 and 48. Similar to the no-friction cases there is a **shift** to the right in the early time plot for lower initial chamber pressures, and the late time response is **not** significantly affected by the initial chamber pressure.

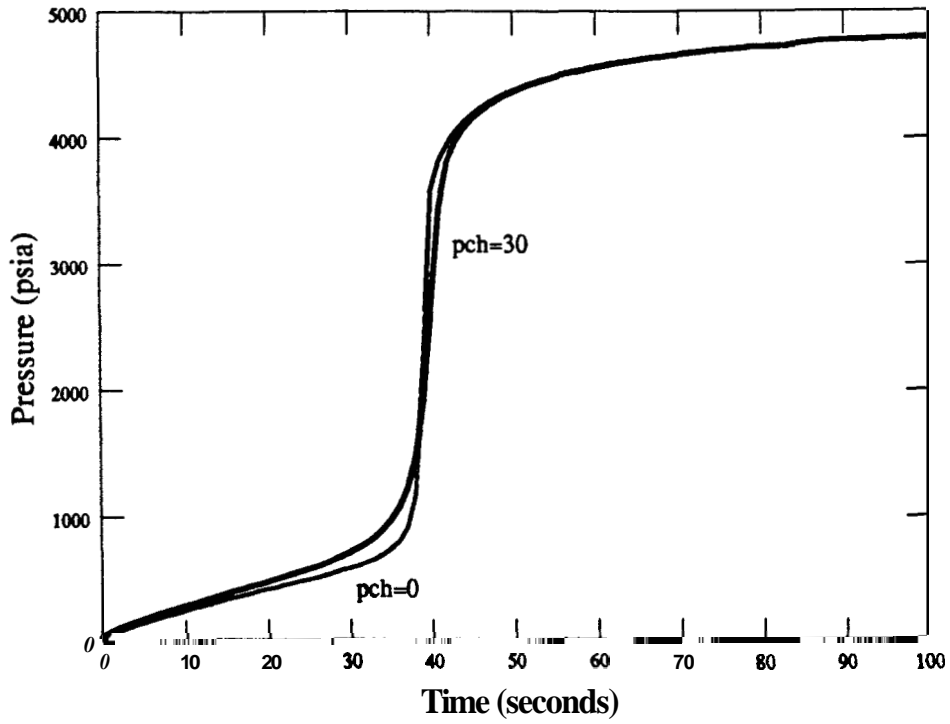


Figure 45: Bottom Hole Pressure for Different Initial Chamber Pressures

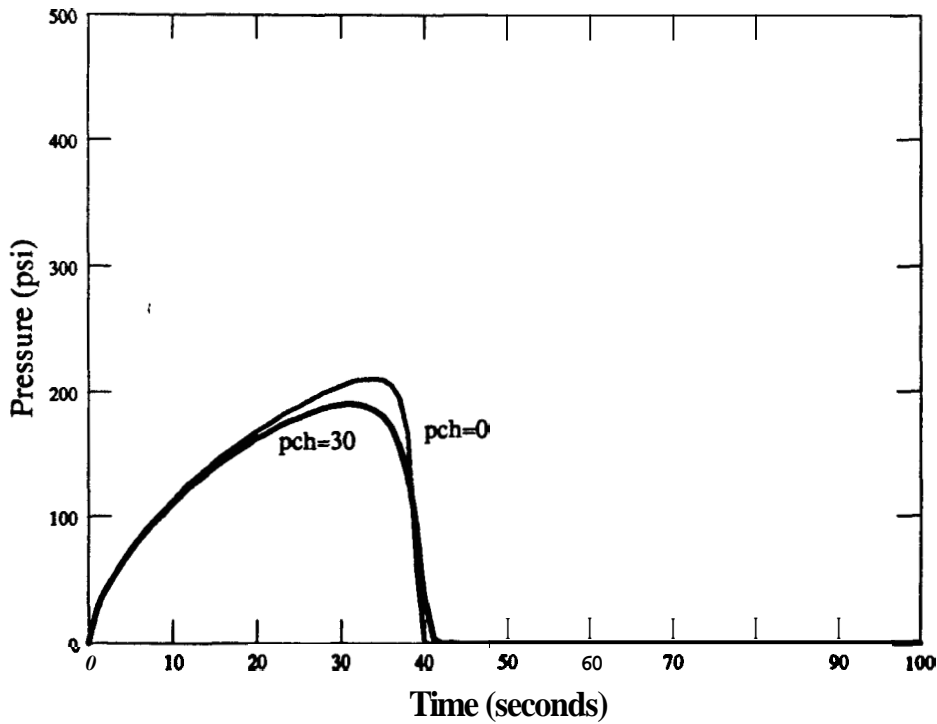


Figure 46: Frictional Pressure Drop for Different Initial Chamber Pressures

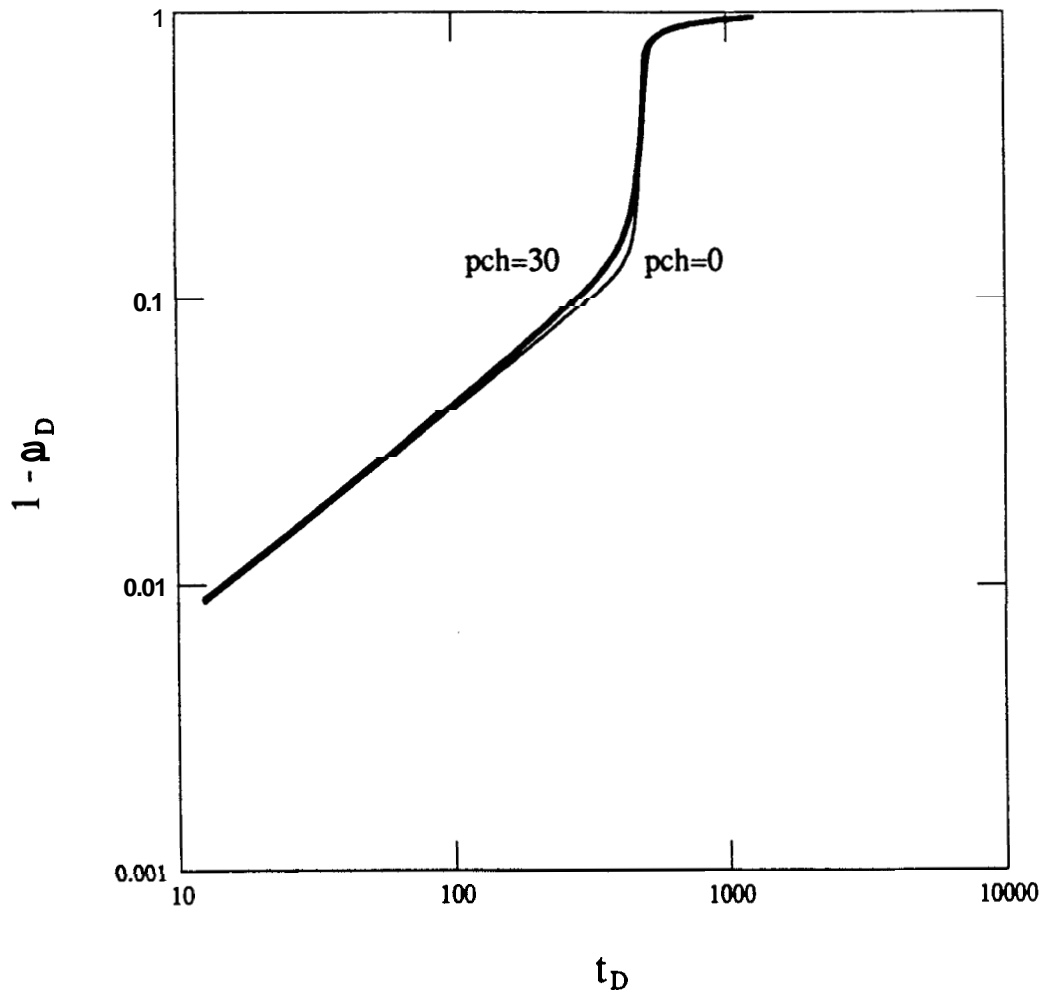


Figure 47: ~~Early~~ Time Plot for Different Initial Chamber Pressures

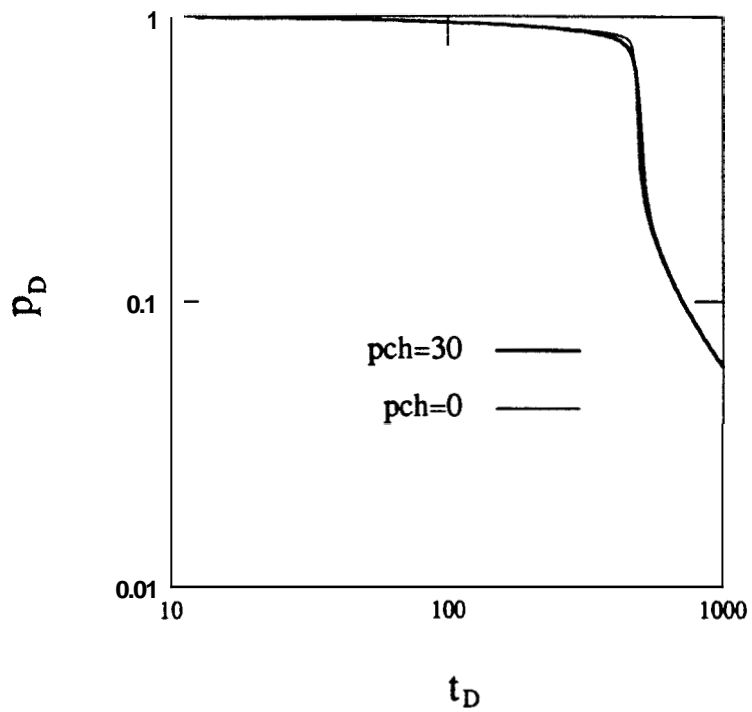


Figure 48: Late Time Plot for Different Initial Chamber Pressures

6. CONCLUSIONS AND RECOMMENDATIONS

In **this** study, frictional effects were included in the closed chamber well test model developed by **Simmons (1985)** in order to develop a more general solution for the closed chamber well test.

According to the results obtained in **this** study, frictional effects significantly affect **the** early time pressure response, while late time pressure responses are not highly affected. The inclusion of tubing frictional losses in the closed chamber test acts like a choke, and reduces the instantaneous flowrate into the wellbore. However, at early time, when **the** bottom hole pressure is not affected by the pressure in the chamber, the presence of frictional effects increase the bottom hole pressure in comparison to the frictionless case. **The** gas compression in the chamber **is** only a function of the liquid level, (no mass transfer between the liquid column and the chamber **gas**). Since the flowrate is restricted by the tubing friction, the liquid levels are lower than in the frictionless case, and the rapid compression of the chamber gas is delayed. Hence, the late time bottom hole pressure for the friction case is lower than the bottom hole pressure for the frictionless case.

A sensitivity study was performed to analyze the influence of different tool and reservoir parameters on the closed chamber well test including frictional effects. The frictional pressure drop is closely related to the tool parameters like chamber diameter, absolute roughness and chamber length. Frictional losses could be reduced by controlling these parameters. For **instance**, for large chamber diameters the friction pressure losses become small enough such that the total pressure response **is** practically unaffected.

In general, the frictional pressure loss during a closed chamber test increases rapidly, levels off **as** it goes through a maximum, and finally decreases rapidly **as** the chamber gas compresses and chokes the well. We observe that as the frictional effects increase, the **durations of** significant frictional head losses decrease. **This** reduction in the durations of the **frictional** effects is observed when we compare closed chamber **tests** with different diameters, different initial **reservoir** pressures **and** different wellbore **skins**.

As expected, the sensitivity study showed that the early time responses in the presence of wellbore skin differ significantly from early time responses without wellbore skin. In log-log format the early time response without wellbore skin is similar to the slug test response with a **slope** of $1/2$ denoting transient linear flow. On the other hand, the early time log-log response with wellbore skin **has** a unit slope, representing constant flowrate. The flowrate profile in the presence of high wellbore skin is practically constant, and decreases rapidly like a shut-in. Hence, the late time build-up could be approximated as a simple build-up flowing a constant rate flow period, and analyzed using a Homer technique.

The closed chamber well test model developed by **Simmons** was also improved by using variable time steps instead of a fixed time step. With variable time steps the computer time is reduced significantly because the number of computations is reduced by an order of magnitude in comparison to the calculations required when using fixed time steps. The program with variable time steps should be improved by including a restarting routine such that the program could be restarted from a given time greater than **zero**.

Momentum effects of the fluid between the lower valve and the formation, and in the cushion above the lower surge valve, were not considered in the model. Momentum effects are important in the cases where high flowrates occur and the initial fluid column in the wellbore must accelerate rapidly. **For** this reason it is recommended to include momentum effects on the closed chamber well test.

In developing the model, it is also assumed that wellbore liquids are incompressible. The late time response depends significantly on the high pressure compressibility of the gas. Yet, at these high pressures, the volume of the gas is small. On the other hand, the liquid column compressibility is low, but its volume is large. The wellbore storage is a function of the two fluid columns in the wellbore. Hence, future studies should analyze the influence of the produced liquid compressibility on the closed chamber pressure response.

Summary

1. Frictional effects were included in the superposition model for the closed chamber well test.
2. Frictional effects significantly affect the early time pressure response, whereas the late time pressure response is not highly affected.
3. **As** the frictional effects increase, the durations of significant frictional head losses decrease.
4. Early time responses in the presence of wellbore skin differ significantly from early time responses without wellbore **skin**.
5. The flowrate profile in the presence of **high** wellbore skin is practically constant, and decreases rapidly like a shut-in. Hence, the late time build-up with high wellbore skin could **be** approximated as a simple build-up flowing **a** constant rate flow period, and analyzed using a conventional Horner technique.

Recommendations for Future Studies

1. Consider the effect of momentum effects on the closed chamber well test.
2. Analyze the influence of the produced liquid compressibility on the closed chamber pressure response.
3. Improve the superposition model with variable time steps by including a restarting routine.

NOMENCLATURE

- A_{ch} = Cross sectional area of the chamber (ft^2)
- c_t = ~~Total~~ formation compressibility (psi^{-1})
- D = Inside pipe diameter (ft)
- D_{ch} = Chamber diameter (ft)
- e = Absolute roughness (in)
- e/D = Relative roughness
- f = Moody friction factor
- g = Acceleration of gravity constant ($32.2 ft/sec^2$)
- g_c = Conversion factor ($32.2 lbm-ft/lbf-sec^2$)
- h = Formation thickness (ft)
- h_f = Frictional head loss (ft)
- k = Reservoir permeability (mD)
- K_0 = Modified Bessel function of second kind, zero order
- K_1 = Modified Bessel function of second kind, first order
- L = Pipe length (ft)
- L_c = ~~Total~~ chamber length, as illustrated in Figure 2 (ft)
- L_{ci} = Initial fluid level, as illustrated in Figure 2 (ft)
- N = Time step index
- N_p = Cumulative liquid production (ft^3)
- p_{ch} = Chamber pressure ($psia$)
- p_{ch_i} = Initial chamber pressure ($psia$)
- p_1 = Pressure at point 1, as expressed in Equation (1) (psi)
- p_2 = Pressure at point 2, as expressed in Equation (1) (psi)
- p_D = Dimensionless pressure
- p_i = Static initial reservoir pressure ($psia$)

p_o	Minimum well bore pressure achieved during the test (<i>psia</i>)
p_{wf}	Bottom hole flowing pressure (<i>psia</i>)
Δp	Pressure change (<i>psi</i>)
q	Flowrate (ft^3/sec)
q_o	Oil flowrate (<i>bbl/D</i>)
Q	Cumulative influx (<i>bbl</i>)
Q_D	Dimensionless cumulative influx
\bar{Q}_D	Laplace Dimensionless cumulative influx
r	Radius (<i>ft</i>)
r_w	Wellbore radius (<i>ft</i>)
r_D	Dimensionless radius
Re	Reynolds number
s	Laplace variable
S	Dimensionless skin factor
t	Time (<i>sec</i>)
Δt	Time step (<i>sec</i>)
t_D	Dimensionless time
Δt_D	Dimensionless time step
v	Specific volume ($(lbm/ft^3)^{-1}$)
V	Average fluid velocity (<i>ft/sec</i>)
$\Delta(V^2)$	Change in velocity terms (ft^2/sec^2)
V_{ch}	Chamber gas volume (ft^3)
V_{ch_i}	Initial chamber gas volume (ft^3)
X	Dynamic fluid level, as illustrated in Figure 2 (<i>ft</i>)
Δx	Fluid level change per time step (<i>ft</i>)
z	Elevation (<i>ft</i>)
Δz	Change in elevation (<i>ft</i>)

- $Z =$ Real gas compressibility factor of chamber gas
- $Z_i =$ Initial real gas compressibility factor of chamber gas
- $a =$ Kinetic energy correction term
- $\beta =$ Influx constant (*bb/psi*)
- $\mu =$ Fluid viscosity (*cp*)
- $\mu_o =$ Oil viscosity (*cp*)
- $\phi =$ Formation porosity (fraction)
- $\rho_f =$ Fluid density (*lbm/ft³*)

REFERENCES

- Alexander, L. G.: "Theory and Practice of the Closed Chamber Drillstem Test Method," *J. Per. Tech.*, (December, 1977) **1539-1544**
- Benedict, R. P.: Fundamentals of Pipe Flow ,John Wiley and Sons, Inc., U.S.A., 1980.
- Chatas, A. T.: "A Practical Treatment of Nonsteady-State Flow Problems in Reservoir Systems," *Per. Eng.*, (May, June and Aug., 1953) **Vol. 25**
- Cheremisinoff, N. P.: Fluid Flow: Pumps, Pipes and Channels ,Ann Arbor Science, U.S.A., 1981.
- Cooper, **H. H.** ,Bredehoeft, J. D., and Papadopoulos, I. S.: "Response of a Finite Diameter Well to a Instantaneous Charge of Water," *Water Resources Research*, (1967) **263-269**
- Da Prat, G.: "Well Test Analysis for Naturally Fractured Reservoirs," *Ph. D. Dissertation*, Stanford University, July 1981.
- Ferris, J. C., and Knowles, D. B.: "The Slug Test for Estimating Transmissibility of an Aquifer," *U.S. Geol. Survey Ground Water Note 26* ,(1954) **1-7**
- Marshall, G. R.: "Practical Aspects of Closed-Chamber Testing," *J. Cdn. Per. Tech.*, (September, 1978) **82-85**
- Moody, L. F.: "Friction Factors for Pipe Flow," *Tram. A.S.M.E.*, (November, 1944) **671-684**
- Ramey, **H. J.**, and Agarwal, R. G.: "Annulus Unloading Rates as Influenced by Wellbore Storage and Skin Effect," *Soc. Per. Eng. J.*, (October, 1972) **453-462**
- Ramey, **H. J.**, Agarwal, R. G., and Martin, I.: "Analysis of "Slug Test" or DST Flow Period Data," *J. Cdn. Pet. Tech.*, (July, 1975) **37-47**
- Sageev, A.: "Slug Test Analysis," *Water Resources Research*, (1986)
- Saldana, M.: "Flow Phenomenon of Drill Stem Test with Inertial and Frictional Wellbore Effects," *Ph. D. Dissertation*, Stanford University, October, 1983.
- Shinohara, **K.**: "A Study of Inertial Effect in the Wellbore in Pressure Transient Well Testing," *Ph. D. Dissertation*, Stanford University, April, 1980.
- Simmons, J.: "Closed Chamber Well Test Analysis by Superposition of the Constant Pressure Cumulative Influx Solution to the Radial Diffusivity Equation," *M. S. Report*, Stanford University, February, 1985.
- Simmons, J.: "Interpretation of Underbalanced Surge Pressure Data by Rate-Time Convolution," *SPE Paper 15477*. To be presented at the **61st Annual** Technical Conference and Exhibition of the Society of Petroleum Engineers held in New Orleans, LA, Oct. **5-8, 1986**.

Simmons, J., and Sageev, A.: "Application of Closed Chamber *Theory* to Backsurge Completion Testing," *SPE Paper 14252*. Presented at the 60th Annual Technical Conference and Exhibition of the Society of Petroleum Engineers held in Las Vegas, NV, Sept. 22-25, 1985.

APPENDIX 1

COMPUTER PROGRAM

In this appendix the computer program is presented. Since the program for constant time steps is a subset of the program for variable time steps, only the latter one is presented. Also, the program output for the basecase is presented following the computer code.


```

C      *      0 = 00 greater than zero
C      *      1 = 00 less or equal to zero
C      *      N = Total Number of Time Steps
C      *      N1 = Cumulative Number of Time Steps before input
C      *      *      a new time step
C      *      N2 = Number of Time Steps for a given time step
C      *      NAME = Output File Name
C      *      NCOUNT = Counter of Time Steps for a given time step
C      *      NDP = Number of Output Data points
C      *      NLOU = Closest Lower Entry in the Table
C      *      NOUT = Number of Time Steps between output data points
C      *      P = Bottom Hole Flowing Pressure Array (psia)
C      *      PC = Pseudo Critical Pressure (psia)
C      *      PCH = Chamber Gas Pressure (psia)
C      *      PCHI = Chamber Gas Pressure for the previous time step
C      *      PCHI = Initial Chamber Gas Pressure (psig)--->(psia)
C      *      PELEV = Hydrostatic Pressure Drop (psi)
C      *      PERM = Formation Permeability (milli-darcy)
C      *      PFRIC = Frictional Pressure Drop (psi)
C      *      PFRIC1 = Frictional Pressure Drop for the previous time step
C      *      PHI = Formation Porosity (fraction)
C      *      PI = Initial Reservoir Static Pressure (psig)--->(psia)
C      *      PR = Pseudo Reduced Pressure
C      *      qddummy = Dimensionless Cumulative Influx Value Obtained
C      *      *      from Interpolation
C      *      qdtab = Dimensionless Cumulative Influx Values in the
C      *      *      "table" for Interpolation
C      *      Q = Dimensionless Cumulative Fluid Influx Array
C      *      QO = Oil Flowrate (bbl/D)
C      *      QO1 = Oil Flowrate for the Previous Time Step (bbl/D)
C      *      QOTEM = Oil Flowrate for the Previous Time Step (bbl/D)
C      *      RE = Reynolds Number
C      *      RW = Wellbore Radius (ft)
C      *      SGF = Specific Liquid Gravity (relative to water)
C      *      SKN = Hurst Skin Factor
C      *      tddummy = Dimensionless Time
C      *      *      tdtab = Dimensionless Time Values in the Table for
C      *      *      Interpolation
C      *      T = Time Elapsed Array (seconds)
C      *      T1 = Time in which the Pressure Drop is in Effect
C      *      *      Array (seconds)
C      *      TC = Pseudo Critical Temperature (R)
C      *      TEM = Frictional Pressure Drop for the previous time step
C      *      *      TEMP = Chamber Gas Temperature (F)--->(R)
C      *      TR = Pseudo Reduced Temperature
C      *      TT = Total Time (seconds)
C      *      TT1 = Total Time for the previous time step
C      *      UF = Produced Liquid Viscosity (cp)
C      *      *      X = Fluid Level Measured from Mid-Perforations (ft)
C      *      Z = Chamber Real Gas Compressibility Factor
C      *      *      ZI = Initial Chamber Real Gas Compressibility Factor
C      *
C      *      NOTE: Input variable units are "field units" and converted to
C      *      *      absolute units during execution. In the above variable
C      *      *      listing this change in units is denoted as:
C      *      *      (input unit)--->(output unit)
C      *
C      *      SUBROUTINES:
C      *
C      *      FM = Moody Friction Factors Calculation.
C      *      GPC = Pseudo Critical Temperature and Pressure
C      *      *      Calculation for Hydrocarbon Gas.
C      *      GZ = Real Gas Deviation Factor Calculation

```


D = D/12.
ALC = DF - DU
ALI = DF - DB + CL
PCHI = PCHI + 14.696
PI = PI + 14.696
TEMP = TEMP + 460
RW = DW/24
SGF = 141.5/(131.5+API)
ACH = (3.1415926)*(D**2)/4

C

CALL GPC(GG,TC,PC)
TR = TEMP/TC
PR = PCHI/PC
CALL GZ(TR,PR,ZI)

C

T(1) = 0.0
P(1) = PCHI + 0.4333*ALI*SGF
Q(0) = 0.0
B = 1.119*PHI*CT*(RW**2)*H
CDTD = 73.25E-9 *PERM/(PHI*UF*CT*(RW**2))
CQO = 86400
CRE = 1086.08/(UF*D*(131.5+API))
CFH = 4.22E-9*8/((3.1415926**2)*(D**5)*32.174)
CPSI = 0.4333*SGF
CFP = 5.615/ACH
PELEV = CPSI*ALI

C

C

C

C

Output the data check

OPEN(1,FILE=NAME)
WRITE(1,3000)
3000 FORMAT('CLOSED CHAMBER WELL TEST (INCLUDING FRICTIONAL EFFECTS)',
&/.105('*'),///,
&'INPUT DATA AS FOLLOWS:',//)
WRITE(1,3005)NAME
3005 FORMAT('OUTPUT FILE NAME = ',T49,A10,/))
WRITE(1,3010)D
3010 FORMAT('CHAMBER DIAMETER = ',T47,F6.3,' (FEET)')
WRITE(1,3015)E
3015 FORMAT('ROUGHNESS = ',T46,F7.5,' (INCHES)')
WRITE(1,3016)ED
3016 FORMAT('RELATIVE ROUGHNESS = ',T46,F7.5)
WRITE(1,3020)ALC
3020 FORMAT('TOTAL CHAMBER LENGTH FROM PERFORATIONS = ',
&T45,F8.2,' (FEET)')
WRITE(1,3030)ALI
3030 FORMAT('INITIAL FLUID COLUMN LENGTH = ',T45,F8.2,' (FEET)')
WRITE(1,3040)PCHI
3040 FORMAT('INITIAL CHAMBER PRESSURE = ',T45,F8.2,' (PSIA)')
WRITE(1,3045)GG
3045 FORMAT('CHAMBER GAS GRAVITY = ',T47,F6.4,' (AIR=1.0)',/)
WRITE(1,3050)PI
3050 FORMAT('INITIAL RESERVOIR PRESSURE = ',T45,F8.2,' (PSIA)')
WRITE(1,3060)TEMP
3060 FORMAT('RESERVOIR TEMPERATURE = ',T45,F8.2,' (R)')
WRITE(1,3070)SGF
3070 FORMAT('PRODUCED FLUID SPECIFIC GRAVITY = ',T47,F6.4)
WRITE(1,3075)UF
3075 FORMAT('PRODUCED FLUID VISCOSITY = ',T47,F6.3,' (CP)')
WRITE(1,3080)PHI
3080 FORMAT('RESERVOIR POROSITY = ',T47,F6.4)
WRITE(1,3090)PERM

```
3090 FORMAT('RESERVOIR PERMEABILITY = ',T45,F8.2,' (MD)')
WRITE(1,3095)SKN
3095 FORMAT('SKIN = ',T45,F8.3)
WRITE(1,3100)DW/12
3100 FORMAT('WELL DIAMETER = ',T47,F6.4,' (FEET)')
WRITE(1,3110)CT
3110 FORMAT('FORMATION TOTAL COMPRESSIBILITY = ',
&T43,E10.4,' (1/PSI)')
WRITE(1,3120)H
3120 FORMAT('FORMATION THICKNESS = ',T45,F8.2,' (FEET)',)
WRITE(1,3125)
3125 FORMAT(4(//),'NUMBER OF DATA POINTS = ',T50,'100')
WRITE(1,3130)
3130 FORMAT(///,'PRESSURE VS TIME DATA: ',/,105('*'),//,
&5X,'TIME',T17,'Pwf',T25,'FLD PRD',T37,'PELEV',T47,
&'Pch',T57,'Z',T63,'IFLAG',T72,'Re',T81,'f',T91,'qo',
&T101,'PFRIC',/,T3,'(SECONDS)',
&T15,'(PSIA)',T26,'(BBL/D)',T35,'(PSI)',T45,
&'(PSIA)',T89,'(BBL/D)',T99,'(PSI)',/)
WRITE(1,3200)0,P(1),0,PELEV,PCHI,ZI,0,0,0,0,0
C
C *****
C Calculate other initial conditions
C *****
C
Z = ZI
KFLAG=0
FP1 = 0.00
QO1 = 0.00
PFRIC1 = 0.00
TT1 = 0.00
N1 = 0
TEM = 100.00
QOTEM= 100.00
PCHI = PCHI
C
C *****
C Input run data
C *****
C
40 WRITE(6,5000)
5000 FORMAT('TIME STEP? (SECONDS)')
READ(5,*)DT
WRITE(6,5010)
5010 FORMAT('NUMBER OF TIME STEPS? (INTEGER)')
READ(5,*)N2
IF(N2.LT.3)THEN
  DES2 = 'y'
  GO TO 38
ENDIF
WRITE(6,5015)
5015 FORMAT('DO YOU WANT TO CHECK EACH TIME STEP? (y/n)')
READ(5,*)DES2
IF(DES2.EQ.'y')GO TO 38
WRITE(6,5016)
5016 FORMAT('DO YOU WANT TO WRITE THIS SET OF DATA POINTS ?')
READ(5,*)DES3
IF(DES3.EQ.'n')GO TO 38
WRITE(6,5020)
5020 FORMAT('NUMBER OF DATA POINTS ?')
READ(5,*)NDP
NOUT = N2/NDP
C
C *****
```



```
C
C
C
C
C
C
C
C
C
35  CONTINUE
C
C *****
C      The oil flowrate and frictional pressure drop values
C      are checked. If QO is less or equal to zero or FH less
C      than 0.10 ft, the oil flowrate, Reynolds number, Moody
C      friction factor and frictional head loss are set equal
C      to zero.
C *****
C      IF(QOTEM.LE.0.00.OR.TEM.LT.0.10)THEN
C          QO = 0.00
C          FH = 0.00
C          RE = 0.00
C          f = 0.00
C          KFLAG = 1
C          GO TO 36
C      ENDIF
C
C *****
C      The relative roughness value is checked. If ED is equal
C      to zero there are no frictional effects in the tubing,
C      and the frictional head loss is set equal to zero.
C *****
C      IF(ED.EQ.0)THEN
C          FH=0.00
C          GO TO 36
C      ENDIF
C
C ***** Calculate Reynolds Number *****
C      RE = CRE*QO
C ***** Calculate Moody Friction Factor *****
C      CALL FM(RE,ED,F)
C ***** Calculate Frictional Head Loss *****
C      FH= CFH*f*x*(QO**2)
36  CONTINUE
C
C *****
C      Calculate pressure drops and bottom hole pressure
C      (as expressed in Equation (29)).
C *****
C      PELEV = CPSI*X
C      PFRIC = CPSI*FH
C      P(I+1) = PCH + PELEV + PFRIC
C
C *****
C      Print data check
C *****
C      IF(DES2.EQ.'n')GO TO 37
C      WRITE(6,5025) T(I+1),P(I),P(I+1),QO1,QO,PFRIC1,PFRIC,
a  PCH1,PCH
5025  FORMAT('TIME = ',F10.5,/,
a  'P(I) = ',F10.2,2X,'P(I+1) = ',F10.2,/,
a  'QO(I) = ',F10.2,2X,'QO(I+1) = ',F10.2,/,
a  'PFRIC(I) = ',F10.2,2X,'PFRIC(I+1) = ',F10.2,/,
a  'PCH(I) = ',F10.2,2X,'PCH(I+1) = ',F10.2)
```

```
C
C
C *****
C           Ask to repeat last time step
C *****
C
5026 WRITE(6,5026)
      FORMAT('DO YOU WANT TO REPEAT THE LAST TIME STEP ? (y/n)')
      READ(5,*) DES1
C
C ***** Correct counters if the last time step is repeated *****
C
      IF(DES1.EQ.'y')THEN
          N = N1 + NCOUNT - 1
          N1 = N
          DO 12 L=1,I
              T1(L) = T1(L) - DT
12          CONTINUE
          GO TO 40
          ELSE
              DES3 = 'a'
          ENDIF
C
C ***** Actualize cumulative data varlablcs *****
C
37      QO1 = QO
          QOTEM = QO
          FP1 = FP
          PFRIC1 = PFRIC
          PCH1 = PCH
          TEH = PFRIC
C
      WRITE(4,3200)T(I+1),P(I+1),FP,PELEV,PCH,Z,IFLAG,RE,F,QO,PFRIC
C
C *****
C           Selective Data Output
C *****
      IF(DES3.EQ.'n')THEN
          GO TO 10
          ELSE
              IF(DES3.EQ.'y')THEN
                  GO TO 39
                  ELSE
                      IF(DES3.EQ.'a')THEN
7027      WRITE(6,5027)
              FORMAT('DO YOU WANT TO WRITE THIS DATA POINT ?')
              READ(5,*)DES4
              IF(DES4.EQ.'n')THEN
                  GO TO 10
                  ELSE
                      NOUT=1
                      GO TO 39
              ENDIF
              ELSE
                  GO TO 10
              ENDIF
          ENDIF
      ENDIF
C
39      RI = I
          AA = RI/NOUT
          NA = AA
          BB = NA
          IF(AA.NE.BB)GO TO 10
```



```

      F = (1.14-2*DLOG10(Y))**-2
      DIF = DABS(F-F1)
      IF (DIF.LT.1E-6) GO TO 45
40     F1 = F
      CONTINUE
      ELSE
      F = (1.14-2*DLOG10(ED))**-2
      ENDIF
      ENDIF
      ENDIF
C
45  RETURN
   END
C
C
C
C *****
C SUBROUTINE GPC(GG,TC,PC)
C *****
C THIS ROUTINE CALCULATES THE PSEUDOCRITICAL
C TEMPERATURE AND PRESSURE FOR CONDENSATE WELL
C FLUIDS, GIVEN THE GAS GRAVITY. THE EQUATIONS
C USED ARE THOSE GIVEN BY STANDING.
C *****
C IMPLICIT REAL*8(A-H,O-Z)
C
C PC = 706. - 51.7*GG - 11.1*(GG**2)
C TC = 187 + 330*GG - 71.5*(GG**2)
C
C RETURN
C END
C
C
C
C *****
C SUBROUTINE GZ(TR,PR,Z)
C *****
C THIS ROUTINE CALCULATES THE GAS DEVIATION
C FACTOR FOR A NATURAL GAS GIVEN THE REDUCED
C PSEUDOCRITICALS TEMPERATURE AND PRESSURE.
C THE EQUATIONS USED ARE CURVE FIT RELATIONS
C FROM THE STANDING-KAT2 CHART GIVEN BY
C BRILL AND BEGGS.
C *****
C IMPLICIT REAL*8(A-H,O-Z)
C
C A = 1.39*SQRT(TR-0.92) - 0.36*TR - 0.101
C
C B = (0.62 - 0.23*TR)*PR
C &+ (0.066/(TR-0.86) - 0.037)*(PR**2)
C &+ (0.32/(10**(9*(TR-1))))*(PR**6)
C
C C = (0.132 - 0.32*DLOG10(TR))
C
```

```
C      D = 18.**(.3186 - .49*TR +.1824*(TR**2))
C      Z = A + (1-A)/(2.718281828**B) + C*(PR**D)
C      RETURN
C      END
C
C
C      *****
C
C      SUBROUTINE INTERP(tddummy,qddummy,qdtab,tdtab)
C      *****
C
C      THIS ROUTINE INTERPOLATES BETWEEN TWO SUCCESSIVE
C      VALUES IN A TABLE THAT CONTAINS THE DIMENSIONLESS
C      CUMULATIVE INFLUX VALUES FOR DIFFERENT DIMENSIONLESS
C      TIME VALUES.
C      FOR A GIVEN DIMENSIONLESS TIME THE INTERPOLATOR
C      SUBROUTINE COMPUTES THE CLOSEST LOWER ENTRY IN A
C      TABLE, AND INTERPOLATES BETWEEN THIS VALUES AND
C      THE FOLLOWING ENTRY IN THE TABLE.
C      *****
C
C      IMPLICIT REAL*8 (A-H,O-Z)
C      dimension tdtab(550),qdtab(550)
C
C      if (tddummy.lt.0.1) go to 10
C      if (tddummy.lt.1.0) go to 20
C      if (tddummy.lt.10.0) go to 30
C      if (tddummy.lt.100.0) go to 40
C      if (tddummy.lt.1000.0) go to 50
C
C      ***** 1000-10000 RANGE *****
C
C      nlow=460+(tddummy-1000.0)/100.0
C      qddummy=qdtab(nlow)+(qdtab(nlow+1)-qdtab(nlow))*
C      & (tddummy-tdtab(nlow))/100.0
C      go to 999
C
C      ***** 100-1000 RANGE *****
C
C      50 nlow=370+(tddummy-100.0)/10.0
C      qddummy=qdtab(nlow)+(qdtab(nlow+1)-qdtab(nlow))*
C      & (tddummy-tdtab(nlow))/10.0
C      go to 999
C
C      ***** 10-100 RANGE *****
C
C      40 nlow=280+(tddummy-10.0)
C      qddummy=qdtab(nlow)+(qdtab(nlow+1)-qdtab(nlow))*
C      & (tddummy-tdtab(nlow))/1.0
C      go to 999
C
C      ***** 1-10 RANGE *****
C
C      30 nlow=190+(tddummy-1.0)*10
C      qddummy=qdtab(nlow)+(qdtab(nlow+1)-qdtab(nlow))*
C      & (tddummy-tdtab(nlow))/0.1
C      go to 999
C
C      ***** 0.1-1 RANGE *****
```

```
C
20  nlow=100+(tddummy-0.1)*100
    qddummy=qdtab(nlow)+(qdtab(nlow+1)-qdtab(nlow))*
    & (tddummy-tdtab(nlow))/0.01
    go to 999
C
C      ***** 0.01-0.1 RANGE *****
C
10  nlow=1+(tddummy-0.01)*1000
    qddummy=qdtab(nlow)+(qdtab(nlow+1)-qdtab(nlow))*
    & (tddummy-tdtab(nlow))/0.001
C
C      RETURN
999  END
C
C
C
```

APPENDIX 2

**NUMERICAL VALUES FOR THE BASECASE
WITH AND WITHOUT FRICTION**

CLOSED CHAMBER WELL TEST (INCLUDING FRICTIONAL EFFECTS)

INPUT DATA AS FOLLOWS:

OUTPUT FILE NAME = basecase

CHAMBER DIAMETER = 0.203 (FEET)
 ROUGHNESS = 0. (INCHES)
 RELATIVE ROUGHNESS = 0.
 TOTAL CHAMBER LENGTH FROM PERFORATIONS = 1000.00 (FEET)
 INITIAL FLUID COLUMN LENGTH = 0. (FEET)
 INITIAL CHAMBER PRESSURE = 44.70 (PSIA)
 CHAMBER GAS GRAVITY = 0.650 (AIR=1.0)

INITIAL RESERVOIR PRESSURE = 5014.70 (PSIA)
 RESERVOIR TEMPERATURE = 635.00 (R)
 PRODUCED FLUID SPECIFIC GRAVITY = 0.9042
 PRODUCED FLUID VISCOSITY = 1.250 (CP)
 RESERVOIR POROSITY = 0.2700
 RESERVOIR PERMEABILITY = 100.00 (MD)
 SKIN = 0.
 WELL DIAMETER = 0.8333 (FEET)
 FORMATION TOTAL COMPRESSIBILITY = 0.1000e-04 (1/PSI)
 FORMATION THICKNESS = 25.00 (FEET)

NUMBER OF DATA POINTS = 87

PRESSURE VS TIME DATA:

TIME (SECONDS)	Pwf (PSIA)	FLD PRD (BBL/S)	PELEV (PSI)	Pch (PSIA)	Z	Re	f	qo (BBL/D)	PFRI (PSI)
0.	44.70	0.	0.	44.70	0.9964	0.	0.	0.	0.
1.00000	87.68	0.5640	38.17	49.50	0.9960	0.	0.	0.	E.
2.00000	117.04	0.9411	63.70	53.34	0.9957	0.	0.	0.	E.
3.00000	143.87	1.2787	86.55	57.31	0.9954	0.	0.	0.	0.
4.00000	169.48	1.5938	107.88	61.60	0.9950	0.	0.	0.	E.
5.00000	194.46	1.8933	128.15	66.31	0.9946	0.	0.	0.	E.
6.00000	219.18	2.1808	147.62	71.56	0.9942	0.	0.	0.	E.
7.00000	243.93	2.4587	166.43	77.50	0.9937	0.	0.	0.	E.
8.00000	268.98	2.7285	184.69	84.29	0.9932	0.	0.	0.	E.
9.00000	294.59	2.9909	202.45	92.14	0.9925	0.	0.	0.	0.
10.00000	321.16	3.2472	219.80	101.36	0.9918	0.	0.	0.	0.
11.00000	349.14	3.4980	236.78	112.36	0.9909	0.	0.	0.	0.
12.00000	379.09	3.7434	253.39	125.70	0.9898	0.	0.	0.	0.
13.00000	411.83	3.9832	269.62	142.21	0.9885	0.	0.	0.	0.
14.00000	448.71	4.2180	285.51	163.20	0.9867	0.	0.	0.	0.
15.00000	491.78	4.4476	301.62	190.72	0.9845	0.	0.	0.	0.
16.00000	544.50	4.6717	316.22	228.28	0.9814	0.	0.	0.	0.
17.00000	613.06	4.8889	330.92	282.14	0.9769	0.	0.	0.	0.
18.00000	710.08	5.0979	345.07	365.01	0.9699	0.	0.	0.	E.
19.00000	863.46	5.2952	350.43	505.03	0.9582	0.	0.	0.	0.
20.00000	1142.34	5.4729	370.46	771.88	0.9361	0.	0.	0.	0.
21.00000	1702.33	5.6120	379.87	1322.46	0.8956	0.	0.	0.	0.
22.00000	2545.07	5.6846	384.78	2160.28	0.8588	0.	0.	0.	0.
23.00000	3116.22	5.7065	386.27	2729.96	0.8550	0.	0.	0.	E.
24.00000	3419.51	5.7142	386.79	3032.72	0.8596	0.	0.	0.	0.
25.00000	3609.31	5.7181	387.05	3222.26	0.8648	0.	0.	0.	0.
26.00000	3742.41	5.7205	387.22	3355.19	0.8693	0.	0.	0.	0.
26.42000	3792.88	5.7214	387.27	3405.61	0.8712	0.	0.	0.	0.

27.42000	3890.00	5.7229	387.36	3502.62	0.8751	O.	O.	O.	5.
28.42000	3971.80	5.7242	387.46	3564.34	0.8787	O.	O.	O.	O.
29.42000	4041.62	5.7251	387.53	3654.09	0.8619	O.	O.	O.	O.
30.42000	4100.79	5.7259	387.56	3713.20	0.8848	O.	O.	O.	O.
31.55000	4157.94	5.7267	387.63	3770.31	0.8877	O.	O.	O.	e.
32.55000	4203.17	5.7272	387.67	3615.50	0.8901	O.	O.	O.	P.
33.55000	4243.92	5.7277	387.70	3856.22	0.8923	O.	O.	O.	e.
34.55000	4276.60	5.7281	387.73	3888.87	0.8940	O.	O.	O.	O.
35.55000	4309.45	5.7285	387.76	3921.70	0.8959	O.	O.	O.	O.
36.55000	4339.61	5.7288	387.78	3951.83	0.8976	O.	O.	O.	O.
37.55000	4367.56	5.7291	387.80	3979.76	0.8992	O.	O.	O.	e.
38.55000	4389.56	5.7294	387.82	4001.76	0.9005	O.	O.	O.	E.
39.55000	4412.42	5.7296	387.83	4024.58	0.9018	O.	O.	O.	O.
40.55000	4434.22	5.7299	387.85	4046.38	0.9031	O.	O.	O.	O.
41.55000	4454.77	5.7301	387.86	4066.91	0.9044	O.	O.	O.	O.
42.55000	4471.21	5.7302	387.87	4083.33	0.9054	O.	O.	O.	P.
43.55000	4488.35	5.7304	387.89	4100.46	0.9064	O.	O.	O.	e.
44.55000	4504.92	5.7306	387.90	4117.02	0.9074	O.	O.	O.	5.
45.55000	4520.80	5.7307	387.91	4132.90	0.9084	O.	O.	O.	O.
46.55000	4533.27	5.7309	367.92	4145.36	0.9092	O.	O.	O.	e.
47.55000	4546.71	5.7310	387.92	4158.78	0.9100	O.	O.	O.	O.
48.55000	4559.81	5.7311	387.93	4171.88	0.9109	O.	O.	O.	O.
49.55000	4572.48	5.7312	387.94	4184.54	0.9117	O.	O.	O.	O.
50.55000	4582.32	5.7313	387.95	4194.37	0.9123	O.	O.	O.	O.
51.55000	4593.06	5.7314	367.95	4205.11	0.9130	O.	O.	O.	O.
52.55000	4603.72	5.7315	387.96	4215.76	0.9137	O.	O.	O.	e.
53.55000	4614.18	5.7316	387.97	4226.22	0.9143	O.	O.	O.	e.
54.55000	4622.03	5.7317	387.97	4234.06	0.9148	O.	O.	O.	O.
55.55000	4630.89	5.7318	387.98	4242.91	0.9154	O.	O.	O.	e.
56.55000	4639.79	5.7319	387.98	4251.80	0.9160	O.	O.	O.	O.
57.55000	4648.54	5.7319	387.99	4260.55	0.9166	O.	O.	O.	O.
58.55000	4654.97	5.7320	387.99	4266.98	0.9170	O.	O.	O.	O.
59.55000	4662.38	5.7321	388.00	4274.38	0.9175	O.	O.	O.	O.
61.15000	4674.04	5.7322	388.00	4286.03	0.9182	O.	O.	O.	O.
62.05000	4679.36	5.7322	388.01	4291.36	0.9186	O.	O.	O.	5.
63.20000	4687.73	5.7323	388.01	4299.72	0.9191	O.	O.	O.	O.
64.60000	4694.52	5.7324	388.02	4306.51	0.9196	O.	O.	O.	O.
65.10000	4698.56	5.7324	388.02	4310.56	0.9196	O.	O.	O.	O.
65.90000	4703.27	5.7324	388.02	4315.25	0.9202	O.	O.	O.	O.
66.10000	4705.07	5.7324	388.02	4317.05	0.9203	O.	O.	O.	5.
67.10000	4710.31	5.7325	386.03	4322.29	0.9206	O.	O.	O.	O.
68.20000	4716.96	5.7325	388.03	4328.95	0.9211	O.	O.	O.	5.
69.00000	4720.05	5.7326	388.03	4332.02	0.9213	O.	O.	O.	5.
70.00000	4725.22	5.7326	388.04	4337.18	0.9216	O.	O.	O.	5.
71.10000	4731.21	5.7327	388.04	4343.17	0.9220	O.	O.	O.	O.
72.00000	4734.19	5.7327	388.04	4346.15	0.9222	O.	O.	O.	O.
74.60000	4747.76	5.7328	388.05	4359.71	0.9231	O.	O.	O.	O.
75.60000	4748.54	5.7328	388.05	4360.49	0.9232	O.	O.	O.	e.
76.00000	4752.59	5.7329	388.05	4364.54	0.9235	O.	O.	O.	e.
77.20000	4755.72	5.7329	388.05	4367.67	0.9237	O.	O.	O.	O.
78.10000	4758.42	5.7329	388.05	4370.36	0.9239	O.	O.	O.	O.
79.10000	4762.02	5.7329	388.06	4373.96	0.9241	O.	O.	O.	O.
83.35000	4767.55	5.7330	388.06	4379.49	0.9245	O.	O.	O.	O.
83.90000	4775.80	5.7331	388.06	4367.74	0.9250	O.	O.	O.	O.
85.00000	4782.57	5.7331	388.07	4394.50	0.9255	O.	O.	O.	O.
86.00000	4790.11	5.7332	388.07	4402.04	0.9260	O.	O.	O.	O.
87.10000	4798.98	5.7333	388.08	4410.91	0.9266	O.	O.	O.	O.
95.33000	4804.13	5.7333	388.08	4416.05	0.9270	O.	O.	O.	5.
96.00000	4818.13	5.7334	386.09	4430.04	0.9279	O.	O.	O.	O.
101.95000	4820.94	5.7334	388.09	4432.85	0.9281	O.	O.	O.	E.

CLOSED CHAMBER WELL TEST [INCLUDING FRICTIONAL EFFECTS)

INPUT DATA AS FOLLOWS:

OUTPUT FILE NAME = skinØ

CHAMBER DIAMETER = 0.203 (FEET)
 ROUGHNESS = 0.00060 (INCHES)
 RELATIVE ROUGHNESS = 0.00025
 TOTAL CHAMBER LENGTH FROM PERFORATIONS = 1000.00 (FEET)
 INITIAL FLUID COLUMN LENGTH = 0. (FEET)
 INITIAL CHAMBER PRESSURE = 44.70 (PSIA)
 CHAMBER GAS GRAVITY = 0.6500 (AIR=1.Ø)

INITIAL RESERVOIR PRESSURE = 5014.70 (PSIA)
 RESERVOIR TEMPERATURE = 635.00 (R)
 PRODUCED FLUID SPECIFIC GRAVITY = 0.9042
 PRODUCED FLUID VISCOSITY = 1.250 (CP)
 RESERVOIR POROSITY = 0.2700
 RESERVOIR PERMEABILITY = 100.00 (MD)
 SKIN = 0.
 WELL DIAMETER = 0.8333 (FEET)
 FORMATION TOTAL COMPRESSIBILITY = Ø.1ØØØe-Ø4 (1/PSI)
 FORMATION THICKNESS = 25.00 (FEET)

NUMBER OF DATA POINTS = 84

PRESSURE VS TIME DATA:

TIME (SECONDS)	Pwf (PSIA)	FLD PRD (BBL/S)	PELEV (PSI)	Pch (PSIA)	Z	Re	f	qØ (BBL/D)	PFRIC (PSI)
0.	44.70	0.	0.	44.70	0.9964	0.	Ø.	0.	0.
1.ØØØØ	283.72	0.5442	36.83	49.32	0.9960	927830.969	0.015	33995.23	197.57
1.80000	341.04	0.8353	56.54	52.20	0.9958	809004.698	0.015	29641.50	232.ØØ
2.80000	400.46	1.1598	78.50	55.85	0.9955	732644.987	0.015	26843.72	266.18
3.80000	451.10	1.4588	98.74	59.69	0.9952	683599.336	0.015	25046.71	292.67
5.00000	506.16	1.7952	121.51	64.69	0.9948	643016.519	0.016	23559.78	319.05
5.8ØØØØ	540.07	2.0092	136.00	68.33	0.9945	621905.952	0.016	22786.30	335.74
6.80000	579.85	2.2675	153.49	73.32	0.9941	599542.589	0.016	21966.92	353.Ø4
7.80000	617.59	2.5172	170.38	78.88	0.9936	580562.927	0.016	21271.51	368.33
9.20000	669.41	2.8542	193.20	87.87	0.9929	559060.162	0.016	20483.66	388.34
10.20000	706.47	3.0877	2Ø9.Ø1	95.41	0.9923	546435.559	0.016	20021.10	4Ø2.Ø4
11.20000	743.15	3.3157	224.44	104.14	0.9916	535040.940	0.016	19603.61	414.57
12.20000	777.59	3.5382	239.49	114.34	0.9907	523206.796	0.016	19170.01	423.75
13.20000	809.70	3.7557	254.22	126.45	0.9897	510495.392	0.016	18704.28	429.83
14.20000	843.99	3.9688	268.64	141.10	0.9885	499180.416	0.016	18289.70	434.26
15.20000	883.02	4.1776	282.78	159.16	0.9871	489994.049	0.016	17953.12	441.Ø9
16.20000	920.77	4.3817	296.59	181.91	0.9852	478635.336	0.016	17536.94	442.27
17.15000	962.99	4.5716	309.45	209.82	0.9829	468959.733	0.016	17102.43	443.72
18.20000	1Ø18.66	4.7768	323.34	251.52	0.9794	458386.672	0.016	16795.04	443.80
19.40000	1096.53	5.ØØ4Ø	338.72	322.45	0.9735	442938.893	0.016	16229.04	435.36
20.40000	1184.95	5.1858	351.02	416.48	0.9656	425320.050	0.016	15583.50	417.45
21.4ØØØØ	1323.31	5.3584	362.71	575.81	0.9522	400657.387	0.016	14679.87	384.80
22.40000	1581.86	5.5159	373.37	885.37	0.9270	360082.467	0.016	13193.23	323.13
23.40000	2152.23	5.6425	381.94	1574.28	0.8809	273387.370	0.017	10016.77	196.61
24.90000	3203.59	5.7Ø16	386.42	2812.88	0.8543	33920.492	0.020	1242.83	4.29
25.90000	3437.35	5.7137	386.82	3050.42	0.8591	4243.251	0.026	155.47	Ø.11
26.00000	3456.70	5.7150	386.84	3069.85	0.8605	Ø.	Ø.	Ø.	Ø.
27.00000	3656.32	5.7190	387.11	3269.21	0.8663	Ø.	Ø.	Ø.	Ø.

27.82000	3771.27	5.7210	387.25	3384.02	0.8703	0.	0.	0.	0.
28.82000	3880.72	5.7228	387.37	3493.35	0.8747	0.	0.	0.	0.
29.82000	3966.00	5.7241	387.46	3578.54	0.8784	0.	0.	0.	0.
30.82000	4038.44	5.7251	387.53	3650.91	0.8818	0.	0.	0.	0.
31.82000	4100.74	5.7259	387.58	3713.16	0.8848	0.	0.	0.	0.
32.82000	4153.90	5.7266	387.63	3766.27	0.8875	0.	0.	0.	0.
33.82000	4198.22	5.7272	387.67	3810.56	0.8898	0.	0.	0.	0.
34.82000	4239.21	5.7277	387.70	3851.51	0.8920	0.	0.	0.	0.
35.82000	4276.54	5.7281	387.73	3888.81	0.8940	0.	0.	0.	0.
36.82000	4309.98	5.7285	387.76	3922.22	0.8959	0.	0.	0.	0.
37.82000	4338.32	5.7288	387.78	3950.55	0.8975	0.	0.	0.	0.
38.82000	4365.66	5.7291	387.80	3977.87	8.8991	0.	0.	0.	0.
39.82000	4391.41	5.7294	387.82	4003.59	0.9006	0.	0.	0.	5.
40.82000	4414.79	5.7296	387.83	4026.96	0.9020	0.	0.	0.	0.
41.82000	4434.68	5.7299	387.85	4046.83	0.9032	0.	0.	0.	0.
42.82000	4454.57	5.7301	387.86	4066.71	0.9044	0.	0.	0.	0.
43.82000	4473.62	5.7303	387.87	4085.74	0.9055	0.	0.	0.	0.
44.82000	4490.99	5.7304	387.89	4103.10	0.9066	0.	0.	0.	0.
45.55000	4503.55	5.7306	387.90	4115.66	0.9073	0.	0.	0.	0.
46.55000	4517.14	5.7307	387.90	4129.24	0.9082	0.	0.	0.	5.
47.55000	4531.52	5.7308	387.91	4143.60	0.9091	0.	0.	0.	0.
48.55000	4545.58	5.7310	387.92	4157.66	0.9100	0.	0.	0.	0.
49.55000	4559.23	5.7311	387.93	4171.30	0.9108	0.	0.	0.	0.
50.55000	4569.82	5.7312	387.94	4181.88	0.9115	0.	0.	0.	0.
51.55000	4581.19	5.7313	387.95	4193.24	0.9122	0.	0.	0.	0.
52.55000	4592.51	5.7314	387.95	4204.56	0.9129	0.	0.	0.	5.
53.55000	4603.66	5.7315	387.96	4215.69	0.9136	0.	0.	0.	0.
54.55000	4612.03	5.7316	387.97	4224.07	0.9142	0.	0.	0.	0.
56.00000	4626.63	5.7317	387.98	4238.66	0.9151	0.	0.	0.	0.
57.00000	4633.95	5.7318	387.98	4245.97	0.9156	0.	0.	0.	0.
57.98000	4642.28	5.7319	387.99	4254.29	0.9161	0.	0.	0.	0.
58.96000	4650.62	5.7320	387.99	4262.63	0.9167	0.	0.	0.	0.
60.00000	4658.90	5.7320	388.00	4270.91	0.9172	0.	0.	0.	0.
61.15000	4666.17	5.7321	388.00	4278.17	0.9177	0.	0.	0.	0.
62.00000	4672.16	5.7322	388.00	4284.16	0.9181	0.	0.	0.	0.
64.00000	4687.48	5.7323	388.01	4299.47	0.9191	0.	0.	0.	0.
65.10000	4691.47	5.7323	388.01	4303.45	0.9194	0.	0.	0.	0.
66.20000	4699.30	5.7324	388.02	4311.28	0.9199	0.	0.	0.	0.
67.40000	4706.16	5.7325	388.02	4318.14	0.9203	0.	0.	0.	0.
68.00000	4708.82	5.7325	388.03	4320.79	0.9205	0.	0.	0.	0.
69.20000	4714.80	5.7325	388.03	4326.77	0.9209	0.	0.	0.	0.
70.20000	4721.35	5.7326	388.03	4333.31	0.9214	0.	0.	0.	0.
71.30000	4725.94	5.7326	388.04	4337.91	0.9217	0.	0.	0.	0.
71.90000	4730.16	5.7327	388.04	4342.12	8.9220	0.	0.	0.	0.
73.10000	4735.10	5.7327	388.04	4347.06	0.9223	0.	0.	0.	0.
74.20000	4739.87	5.7328	388.04	4351.83	0.9226	0.	0.	0.	0.
75.10000	4743.24	5.7328	388.05	4355.19	0.9228	0.	0.	0.	0.
75.90000	4746.50	5.7328	388.05	4358.46	0.9231	0.	0.	0.	0.
77.50000	4754.65	5.7329	388.05	4366.60	0.9236	0.	0.	0.	0.
78.30000	4757.60	5.7329	388.05	4369.55	0.9238	0.	0.	0.	0.
79.00000	4758.50	5.7329	388.05	4370.45	0.9239	0.	0.	0.	0.
83.45000	4765.97	5.7330	388.06	4377.91	0.9244	0.	0.	0.	0.
84.05000	4773.45	5.7330	388.06	4385.39	0.9249	0.	0.	0.	0.
85.00000	4779.39	5.7331	388.07	4391.32	0.9253	0.	0.	0.	0.
86.15000	4789.62	5.7332	388.07	4401.55	0.9260	0.	0.	0.	0.
87.20000	4796.67	5.7332	388.08	4408.59	0.9265	0.	0.	0.	0.
95.15000	4802.94	5.7333	388.08	4414.86	0.9269	0.	0.	0.	0.
96.00000	4816.57	5.7334	388.09	4428.48	0.9278	0.	0.	0.	0.
102.35000	4818.64	5.7334	388.09	4430.56	0.9280	0.	0.	0.	0.